ELSEVIER

Tectonophysics 265 (1996) 213–238

TECTONOPHYSICS

Synmagmatic folding of the base of the Bergell pluton, Central Alps

C. Davidson [1], C. Rosenberg, S.M. Schmid *

Geologisch-Paläontologisches Institut der Universität, Bernoullistrasse 32, CH-4056 Basel, Switzerland

Received 20 April 1995; accepted 27 March 1996

Abstract

Evidence for magmatic, submagmatic and solid-state deformation in tonalite, granodiorite and country rocks found at the deep-seated floor (22–26 km) of the Bergell pluton demonstrates that final emplacement and crystallization occurred during regional deformation of the pluton and the underlying country rocks. After northward emplacement over the country rocks, but before complete crystallization, the floor of the pluton was folded during simultaneous N–S shortening and E–W stretching. This is evidenced by synmagmatic folds with E–W striking, nearly vertical axial planes, and by regional east-plunging stretching lineations in the country rocks which are parallel to the regional-scale fold axes and the magmatic mineral lineations in the pluton. Opposite senses of shear from the well-foliated, occasionally mylonitic contact suggest that deformation was mostly accomplished by pure shear. Synmagmatic deformation is related to late-stage N–S shortening of the Alpine orogen and shows that the still partially molten pluton responded to low differential stresses very much like the country rocks deformed in the solid-state at high temperatures. Post-emplacement tilting associated with backthrusting along the Insubric mylonites led to the exposure of the pluton's floor at its present-day western margin.

1. Introduction

The intrusion and deformation history of the Bergell pluton and surrounding rocks has been a matter of controversy for at least 100 years (Trommsdorff and Nievergelt, 1983). Much of the controversy has focused on the timing of the intrusion with respect to nappe emplacement and Alpine deformation in general. Trommsdorff and Nievergelt (1983) gave an excellent summary of the historical work in the Bergell Alps, and summarized many of the important field relationships. Because of their work, and from the results of recent geochemical studies (Reusser, 1987; Diethelm, 1989; von Blanckenburg, 1992; von Blanckenburg et al., 1992), many questions surrounding magma generation and evolution, as well as relative and absolute timing have been resolved. In spite of these recent efforts, many questions still remain. These include: (1) What was the regional tectonic setting at the time of intrusion? (2) Was the pluton deformed while partially molten and/or in a solid state? (3) What is the spatial distribution of magmatic and solid state deformation structures? and (4) What is the relation between deformation within the pluton and that of the country rocks?

* Corresponding author. Fax: +41-61-2673-613; e-mail: schmids@ubaclu.unibas.ch

[1] Current address: Department of Geology, Beloit College, Beloit, Wisconsin 53511, USA

0040-1951/96/$15.00 Copyright © 1996 Elsevier Science B.V. All rights reserved.

PII S0040-1951(96)00070-4

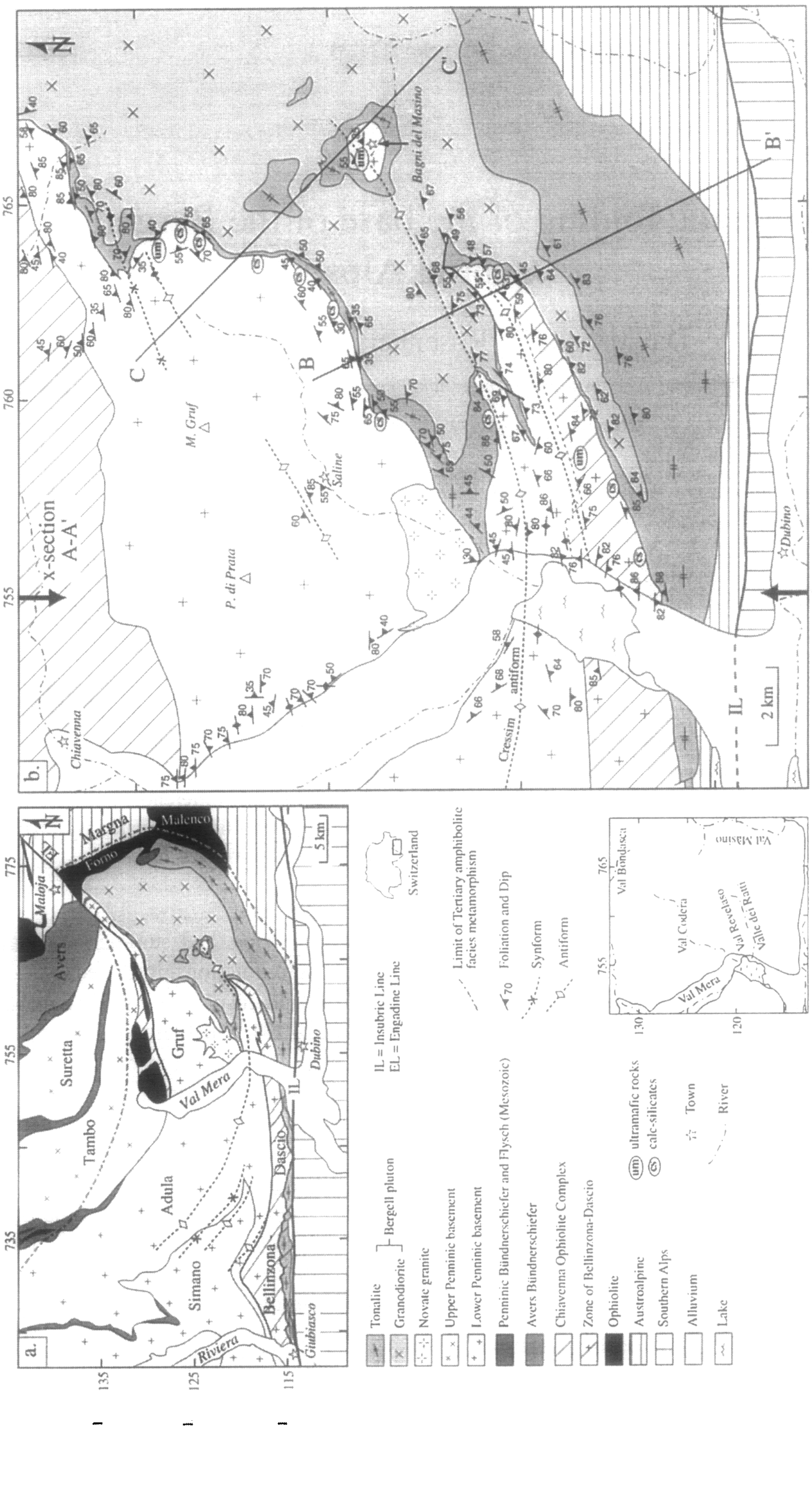

Fig. 1. (a) Tectonic map of the Bergell pluton and vicinity. (b) Geological map of the western contact of the Bergell pluton. Location of cross-sections $A-A'$, $B-B'$ and $C-C'$ shown in Fig. 3 are indicated by arrows ($A-A'$) or solid black lines. Coordinates are Swiss geographical coordinates.

This communication is part of a reinvestigation of the entire Bergell pluton and surrounding rocks which hopes to answer most of these remaining questions (see also Rosenberg et al., 1994, 1995; Berger and Gieré, 1995). In this paper, we present new structural and petrological data from the western contact of the Bergell pluton, present a working hypothesis for the emplacement history of the pluton, and discuss the regional tectonic significance of the intrusion.

2. General geological setting of the Bergell pluton

The Bergell pluton is located along the border of Switzerland and Italy in the Central Alps, near the boundary between the Pennine and Austroalpine Nappes at the eastern edge of the Lepontine dome (Merle et al., 1989) (Fig. 1). Tonalites and granodiorites cooled through their solidus at 32 and 30 Ma, respectively, at the eastern margin (von Blanckenburg, 1992). The pluton is composed primarily of tonalite and granodiorite, with minor amounts of gabbro, hornblendite, aplite and pegmatite (Trommsdorff and Nievergelt, 1983; Diethelm, 1989). It is a composite pluton in that mafic compositions (predominantly tonalite and minor amounts of gabbro and other mafic rock types) form the margins of the pluton with granodiorite occupying the core and northwestern margin. A zone of mingling and mixing is often present between the granodiorite and tonalite ("Übergangszone" of Moticska, 1970; Wenk and Cornelius, 1977) and is best developed in the west. In the east, cross-cutting relationships between tonalite and granodiorite demonstrate the slightly younger crystallization age of the granodiorite in this part of the pluton (Trommsdorff and Nievergelt, 1983; Berger and Gieré, 1995), consistent with radiometric dating (von Blanckenburg, 1992).

The phases present in the tonalite are predominantly plagioclase, quartz, hornblende and biotite, little epidote and K-feldspar (Reusser, 1987). Granodiorite mainly contains plagioclase, quartz, K-feldspar and biotite, and little hornblende (Reusser, 1987). K-feldspar megacrysts are usually present in the granodiorite (3–5 cm, but sometimes > 10 cm) as well as in the "Übergangszone". The presence of these megacrysts allows for easy identification of the granodiorite in the field, and simplyfying, we mapped plutonic rocks from the Bergell pluton which contain K-feldspar megacrysts (including rocks of the "Übergangszone") as granodiorite in Fig. 1.

To the west of the main body of the pluton, a steeply inclined tabular body of tonalite (informally referred to as the tonalite tail) extends almost to Giubiasco near Bellinzona (Fig. 1a). This tonalite tail is part of the Southern Steep Belt (Milnes, 1974), a zone of steeply north-dipping (60–90°), well-foliated rocks, bounded by the Insubric mylonites at its southern margin (Fig. 1). The Insubric line is a major shear zone present in the Central Alps with a long history of movement. The oldest fabrics present in the shear zone formed during ductile shearing with north-side up displacements, followed by later dextral strike-slip motion (Schmid et al., 1987, 1989; Heitzmann, 1987). These mylonites are cut by the younger brittle Insubric fault, a dextral strike-slip fault (Fumasoli, 1974; Schmid et al., 1987). North-side up movement along the Insubric shear zone, in combination with rapid erosion, appears to be responsible for the rapid exhumation of the high-grade metamorphic rocks of the Lepontine dome and Bergell pluton during Late Oligocene times (Hurford, 1986; Heitzmann, 1987; Schmid et al., 1989). Rosenberg et al. (1994, 1995) show that intrusion of the tonalite tail occurred during early stages of backthrusting, and suggest that the tail is a remnant of the feeder system of the main body of the Bergell pluton.

The rock types and metamorphic conditions within the tectonic units into which the pluton was emplaced, vary dramatically from west to east. In the west, the pluton intruded the high-grade, migmatitic ortho- and paragneisses of the Gruf complex, a part of the lower Penninic Adula nappe of the Lepontine dome (Fig. 1a). No contact aureole is present in these rocks, suggesting that temperatures in this region were high (upper-amphibolite to granulite facies conditions) at the time of intrusion. High country-rock temperatures in the west at the time of intrusion are also supported by young (syn- to post-Bergell) isotopic dates from high-temperature geochronometers (Hunziker et al., 1992).

In the east, the pluton intrudes ultramafic and mafic rocks of the Forno and Malenco units (Trommsdorff and Nievergelt, 1983; Berger and Gieré, 1995). The main episode of regional metamorphism and deformation in the Austroalpine rocks east of the pluton is Cretaceous and predates the intrusion by several tens of Ma (Spillmann, 1993; Hunziker et al., 1992). At the time of the intrusion these rocks were at greenschist facies conditions and were contact metamorphosed to approximately 700°C at 3 kbar at the pluton margin (Trommsdorff and Evans, 1972, 1977).

Many lines of evidence suggest that the present-day outlines of the pluton in map view represent a distorted vertical cross-section at the time of emplacement. Due to the pronounced easterly plunge of all structures and rock units which formed after final emplacement, deeper levels of the pluton are exposed in the west, and shallower levels are exposed in the east. In addition to the contrasting nature of metamorphism in the country rocks (regional vs. contact metamorphism) from west to east, evidence for post-emplacement tilting of the pluton includes: (1) asymmetric distribution of Alpine-age metamorphic Al_2SiO_5 around the pluton (Wenk, 1992); (2) Al-in-hornblende barometry from tonalite of the pluton (Reusser, 1987; this study); (3) trend of isotopic dates (Villa and von Blanckenburg, 1991; Hunziker et al., 1992) and (4) paleomagnetic data (Rosenberg and Heller, submitted).

3. Map-scale structures along the western contact

Tonalite is present all along the western contact, with two notable exceptions in upper Val Codera and in Valle dei Ratti (Fig. 1b) where the "Übergangszone" is in direct contact with the country rocks. The tonalite has a well-developed foliation defined by the preferred orientation of biotite and plagioclase laths, and/or lineation defined by the alignment of elongate hornblende crystals. Near the contact the "Übergangszone" and the granodiorite usually also have a well-developed foliation marked by the preferred orientation of biotite, while the alignment of K-feldspar megacrysts defines a mineral lineation. Foliations and lineations along the western margin of the pluton are allways concordant with those of the surrounding rocks (Fig. 2). Foliation orientation varies along the contact because the contact was subsequently folded while the lineation directions consistently plunge about 30° to the east. Mineral lineations within the pluton near the contact represent stretching lineations since they are parallel to the long axes of deformed mafic enclaves. Also shown in Fig. 2 are the calculated fold axes (stars) from best fitting great circles to the plotted foliations. In general, these fold axes plunge about 30° to the east, hence parallel to the stretching lineations. Within the country rocks of Valle dei Ratti in the south (Fig. 2c), however, mesoscopic-scale fold axes from isoclinal, parasitic folds are extremely variable and plot on a single south-dipping girdle which is parallel to the axial plane of a large antiform present in Valle dei Ratti. This suggests curving fold axes associated with very large strains which led to the formation of this high-amplitude antiform (Fig. 3b). A locally shallow westerly plunge is observed in area *b* of Fig. 2.

3.1. Adula–Gruf unit

The Bergell pluton overlies high-grade migmatitic rocks along its entire western border. In the north, these rocks largely belong to the Gruf complex, and in the south (Valle dei Ratti, Fig. 1), they belong to the zone of Bellinzona–Dascio. The Gruf complex is predominantly composed of migmatitic quartz–feldspathic orthogneiss. On a regional scale, the term "Adula–Gruf unit" is used because the Gruf complex is in structural continuity with, and lithologically identical, to the southern part of the Adula nappe exposed west of Val Mera, and to the rocks below the pluton exposed in a window at Bagni del Masino (see Fig. 1b). The orthogneisses and paraschists of the Gruf complex usually have a well-developed foliation defined by the preferred orientation of biotite. Stretching lineations, defined by trails of biotite aggregates and/or aligned metamorphic minerals in paraschists (e.g., sillimanite needles), are present on some foliation surfaces. Upper-amphibolite to granulite metamorphic grade prevails within the Gruf complex, hence no contact metamorphic effect from the Bergell pluton is recorded (Bucher-Nurminen and Droop, 1983; Droop and Bucher-Nurminen, 1984).

3.2. *Remnants of a former nappe boundary at the immediate contact*

Amphibolites, ultramafic rocks, and calc-silicates are largely found concentrated within a discontinuous narrow zone (Diethelm, 1989), directly underlying the pluton along its western margin (Fig. 1b). The same characteristic rock association also crops out directly below the intrusion in the window at Bagni del Masino (Hansmann, 1981) and is typical for parts of the zone of Bellinzona–Dascio (Fig. 1a). This zone is presently found south of the Adula–Gruf unit and within the Southern Steep Belt. West of Val Mera, the zone of Bellinzona–Dascio originally must have overlain the Adula–Gruf unit, because the contact was later backfolded around the Cressim antiform (Hänny et al., 1975; Heitzmann, 1975; Hafner, 1993) into its present steeply north-dipping attitude. East of Val Mera and in Valle dei Ratti, a distinction between the Adula–Gruf unit and the zone of Bellinzona–Dascio is difficult to make, due to a gradual transition from predominant orthogneisses (Adula–Gruf unit) to predominant paraschists (Be-

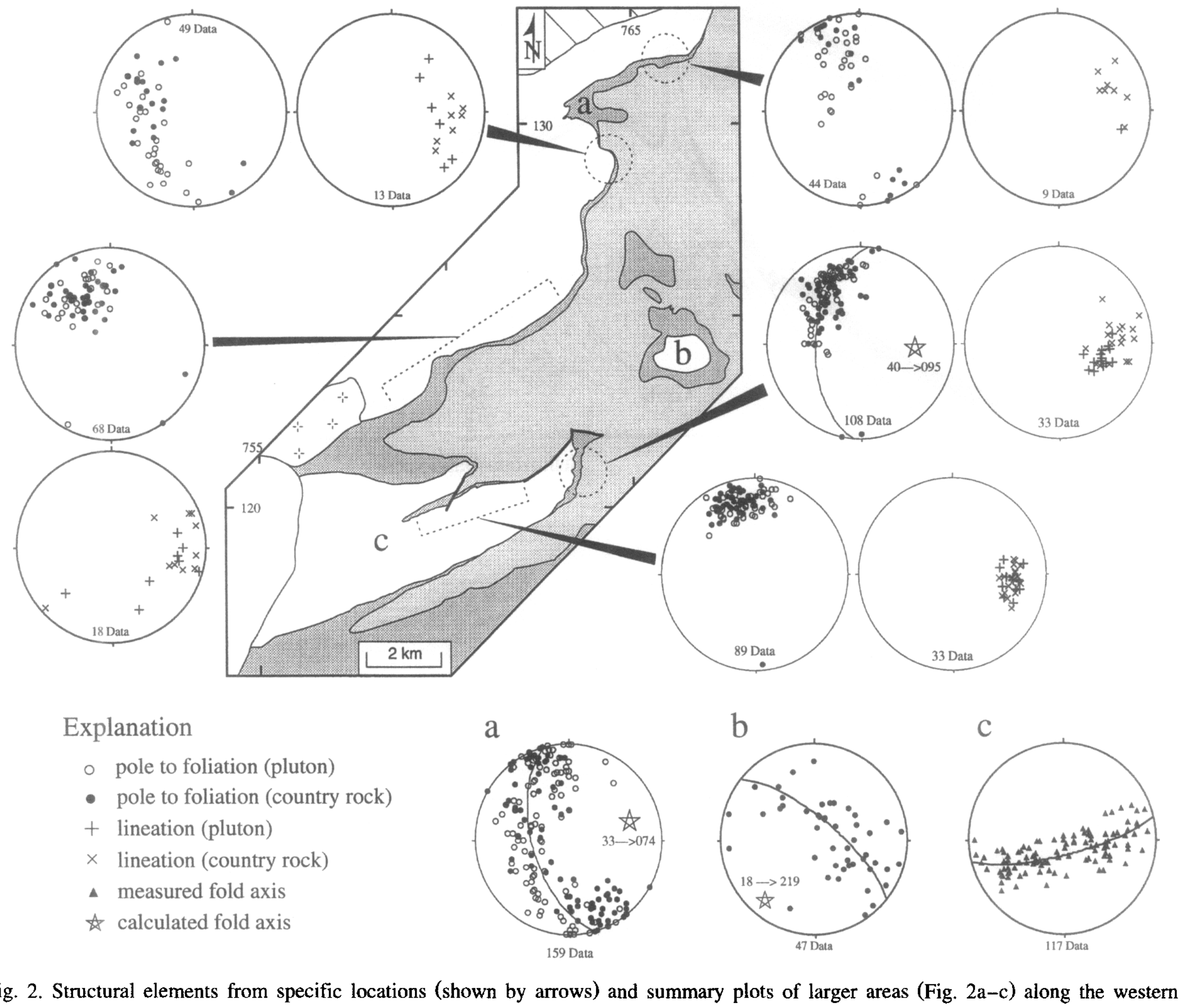

Fig. 2. Structural elements from specific locations (shown by arrows) and summary plots of larger areas (Fig. 2a–c) along the western contact of the Bergell pluton. Stereonets are lower hemisphere equal-area projections: note the concordance of foliations and lineations in the pluton and country rocks. (a) Foliations from the northern part of the western contact (north of Swiss grid latitude 128) folded by the Codera antiform and synform (Fig. 1b). The calculated fold axis (star) plunges 33° ENE and is roughly parallel to mineral and stretching lineations in the area. (b) Foliations from a single mesoscopic anticline from Bagni del Masino. The calculated fold axis (star) gently plunges to the SW. (c) Measured fold axes from mesoscopic parasitic folds with extremely variable trends and plunges found in the Gruf complex in Valle dei Ratti. These fold axes plot on a single south-dipping girdle defining the axial plane of the large-scale antiform in Valle dei Ratti (Fig. 1b), suggesting they formed together.

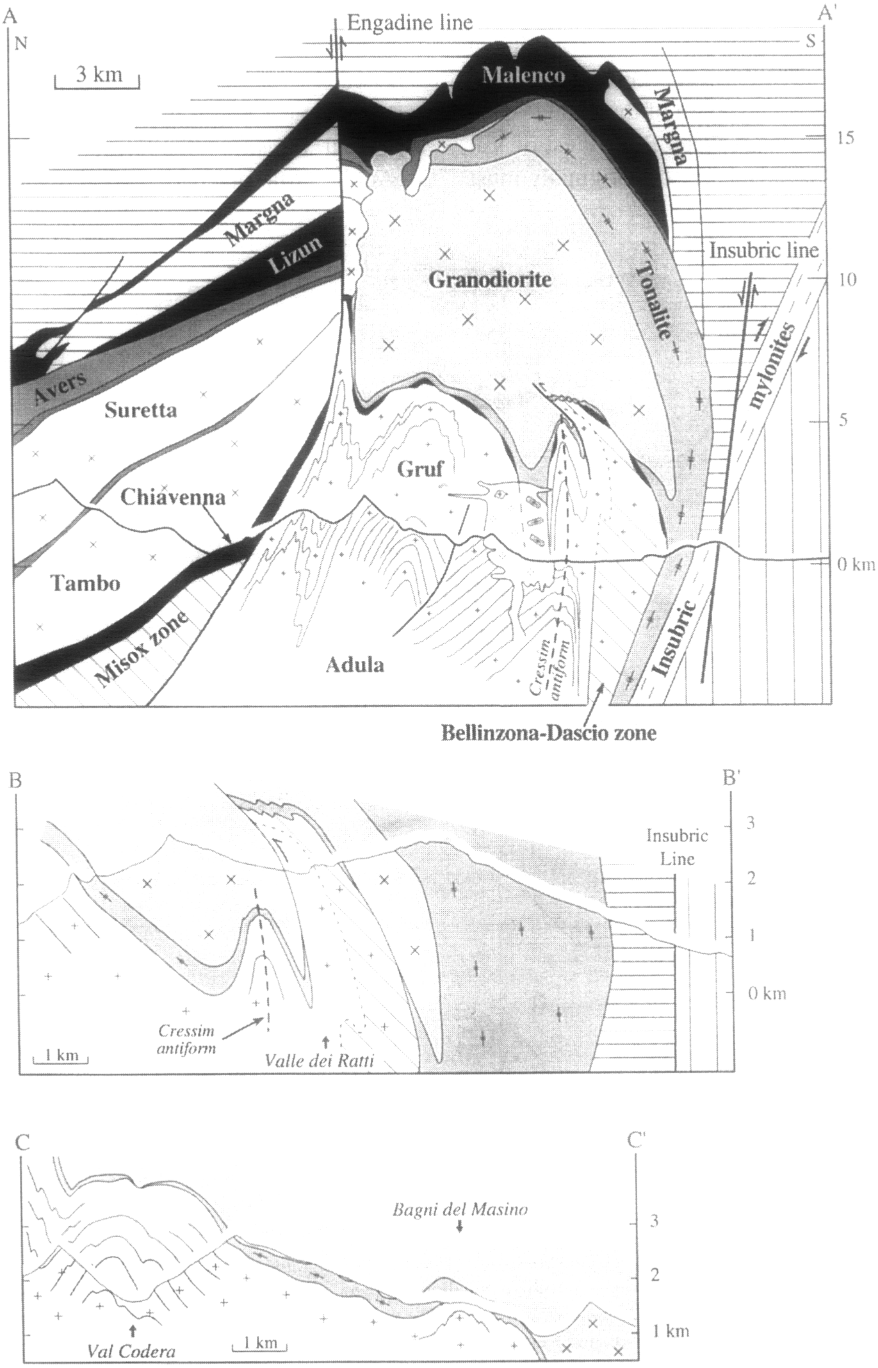

Fig. 3. Cross-sections from the Bergell pluton (see Fig. 1 for location). Section A–A' is modified from Schmid et al. (1996). Note the shear zone in section B–B' (half arrow above the topography) which offsets the tonalite and dies out into homogeneous granodiorite. The Val Codera and Bagni del Masino antiforms are shown in section C–C'.

llinzona–Dascio zone), with calc-silicates and ultramafic rocks again concentrated in a zone directly adjacent to the pluton.

In the north, the Adula–Gruf unit is in contact with the structurally higher rocks of the Chiavenna ophiolite complex (Schmutz, 1976) along a steeply north-dipping fault zone (Fig. 3a). Mylonitic schists and gneisses define this boundary, and a steep metamorphic field gradient is observed in the rocks of this ophiolite complex which contains ultramafic and mafic rocks, pelitic schists and calc-silicates (Schmutz, 1976). Since this complex originally also structurally overlied the Adula–Gruf unit, a connection to the band of amphibolites, calc-silicates, and ultramafic rocks at the top of the Gruf complex further to the south, and ultimately to the zone of Bellinzona–Dascio, is very probable. This supports a suggestion made by Diethelm (1989), namely that the band of ultramafic, mafic and calc-silicate rocks present along the contact of the Bergell pluton represents a former nappe boundary. According to Schmid et al. (1996) this nappe boundary does represent the suture of the North-Penninic ocean, the Misox zone, separating the Adula–Gruf unit from the Tambo nappe (Fig. 1a). Fig. 3a shows that the Bergell intrusion presently occupies the same structural level taken by the Tambo and Suretta nappes further north.

3.3. Folding of the country rocks and the base of the pluton

Structure-contour maps of the country rock, tonalite, and granodiorite contacts are shown in Fig. 4. These maps were used to construct the cross-sections shown in Fig. 3. The maps and cross-sections show that the country rocks at the western pluton contact generally dip to the southeast underneath the pluton and are exposed again in the erosional window at Bagni del Masino (Fig. 1b). Large (map)-scale upright antiforms and synforms refold this contact (Figs. 1–4).

On a regional scale, the axes of these folds change in strike from NW–SE west of Val Mera to E–W and ENE–WSW in the east (Fig. 1a). One of these large-scale antiforms, the Cressim antiform described by Hänny et al. (1975), Heitzmann (1975) and Hafner (1993), can be traced all the way from west of Val Mera into the folded base of the pluton east of Val Mera. The Cressim fold west of Val Mera represents a classical backfold, refolding the Adula nappe into the Southern Steep belt. It was traced across Val Mera into Val Revelaso (Fig. 1a) and finally into the erosional window of Bagni del Masino (for location see axial trace mapped in Fig. 1b, also compare the structure contours in Fig. 4).

Other large antiforms with near-vertical axial planes are present in Val Codera and Valle dei Ratti (Figs. 1 and 3), their axial traces following the valley floors. The southernmost antiform in Valle dei Ratti is associated with a thrust, which displaces the tonalite rim of the intrusion contact by some 2 km along the northern strongly attenuated limb of this mega-fold (half-arrow in Fig. 3b).

Previous workers traced the Cressim antiform either into the antiform in Valle dei Ratti (Heitzmann, 1975) or that in Val Codera (Moticska, 1970; Wenk, 1973). While we disagree with both these correlations, it is clear that important geometrical changes in the fold geometry occur across Val Mera and further to the east: The amplitude of the Cressim antiform decreases eastward, while at the same time much of the N–S shortening is taken up by the Valle dei Ratti antiform east of Val Mera, both antiforms having formed contemporaneously.

4. Evidence for magmatic, submagmatic and solid state deformation associated with folding and thrusting

Evidence for magmatic, submagmatic and solid state flow within the pluton margin is found along the entire length of the western contact. There, magmatic flow commonly results in fabrics (e.g., foliation, lineation) and microstructures which formed while the rock was above its rheological critical melt percentage (Arzi, 1978); that is, before a relatively solid framework developed within the rock during cooling and crystallization and therefore when crystals may easily rotate and orientate in their liquid matrix without internal strain features. Diagnostic for submagmatic flow is microstructural evidence for solid state deformation of crystals in the presence of the last melts, i.e. before complete solidification.

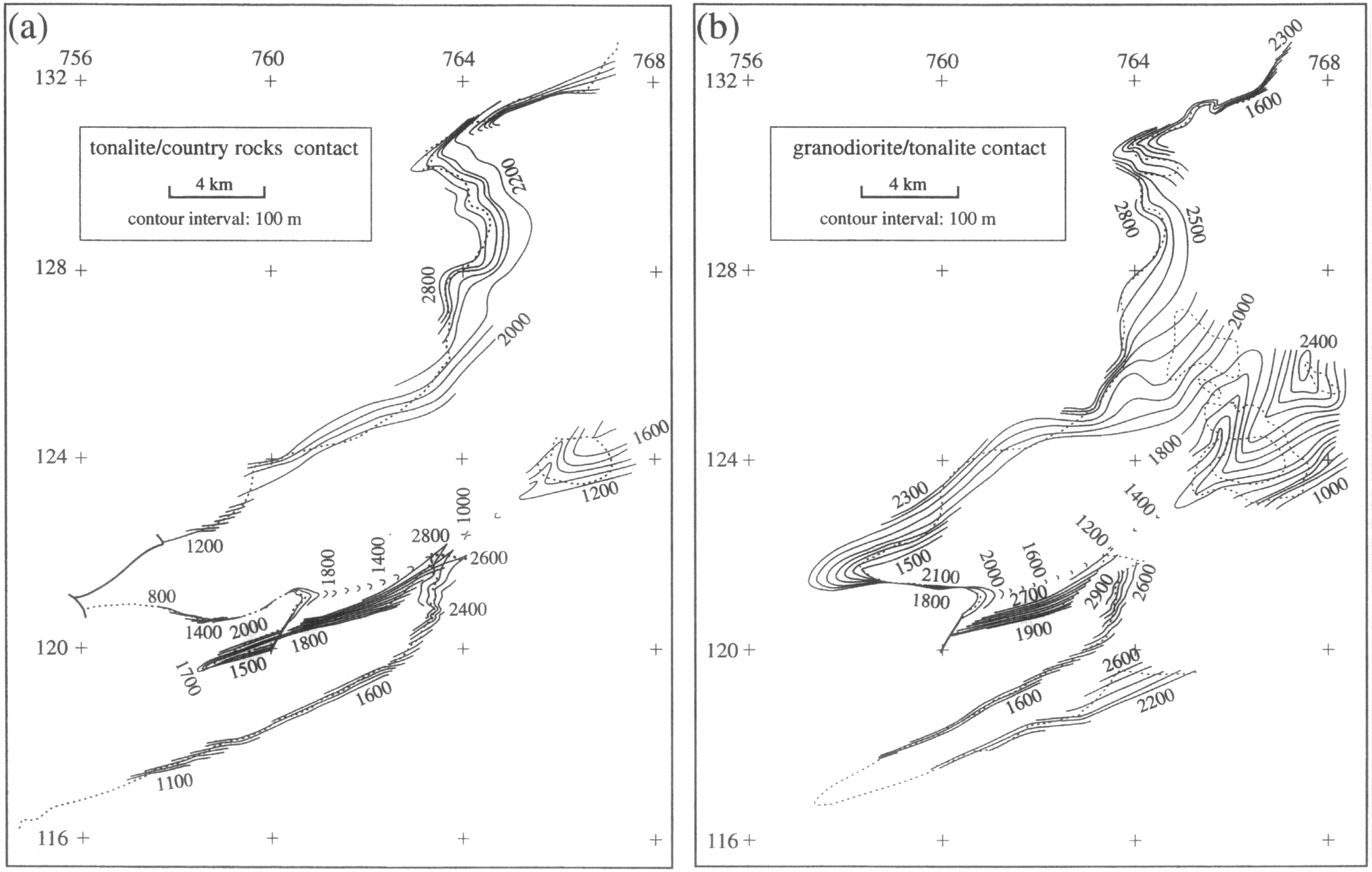

Fig. 4. Structure contour maps of (a) the contact between tonalite and country rocks and (b) the contact between granodiorite (including the "Uebergangszone") and tonalite. Contacts are shown as dotted lines.

This terminology closely follows that used by Bouchez et al. (1992), Guineberteau et al. (1987) and Paterson et al. (1989). Of course, fabrics produced during each of the above stages during progressive deformation may be present the same specimen.

4.1. Foliation and lineation at the pluton margin

Within the interior of the pluton the macroscopic foliation is generally weak and the results from magmatic flow. But, as already described by Wenk (1973) a small amount of solid state overprint is often visible in the microstructure. The following descriptions regard the western margin of the pluton, where foliation is more pronounced. Here, magmatic and submagmatic fabrics, consisting of a contact-parallel foliation and an east-dipping lineation (Fig. 2) are very commonly preserved up to the contact with the country rock.

Magmatic fabrics in tonalite are defined by shape preferred orientations of hornblende, plagioclase laths and biotite. In granodiorite, magmatic fabrics are best marked by a shape preferred orientation of K-feldspar megacrysts (Fig. 5a). However, rocks with little or no submagmatic and/or solid-state deformation are relatively uncommon. These are coarse-grained, the majority of minerals showing no evidence of internal deformation.

Very common is microstructural evidence for submagmatic flow, overprinting the magmatic fabric. In such rocks, K-feldspar megacrysts, plagioclase laths and hornblende are bent, broken, or have fractures filled with plagioclase, quartz, $\pm$epidote (Fig. 6a, see also Bouchez et al., 1992). These fractures, most common in K-feldspar megacrysts and plagioclase, are typically confined to larger single crystals, and they do not extend beyond the edge of the crystal. Occasionally, two, and rarely three, crystals in mutual contact contain a single through-going mineral filled fracture. In addition, phases filling the fractures are usually coarser-grained than those in the matrix and show no evidence of intra-crystalline deformation. The observations that magmatic phases infill the fractures, and that fractures are isolated to single crystals, demonstrate that these fractures formed before complete crystallization of the rock by melt-enhanced embrittlement (Davidson et al., 1994). Subsequent subsolidus overprint in such rocks is often restricted to grain-size reduction and intracrystalline deformation in the matrix minerals, the minerals filling the fractures of large feldspars being unaffected. Host crystal and fracture appear to have behaved as a single rigid particle during subsequent solid state overprint.

Evidence for high-temperature solid-state deformation is common at the pluton margin and includes dynamic recrystallization of plagioclase and quartz, and cataclastic deformation of hornblende (Fig. 6b and c) and K-feldspar. However, in most cases the amount of strain accommodated in the solid-state is minor and such strain features tend to be localized in distinct microstructural sites, for example, between closely spaced megacrysts, or plagioclase phenocrysts (Fig. 6d). Dynamically recrystallized quartz is present in some of these rocks. However, solid state flow of quartz is generally confined to isolated pods within a thin section, and does not lead to the formation of interconnected weak layers (quartz ribbons).

In only a few places, and restricted to the last few meters from the contact, solid state overprint is very intense. Such intensely solid-state deformed tonalites or granodiorites have mylonitic foliations defined by layers of biotite, plastically deformed quartz and feldspar, and cataclastically deformed hornblende (e.g., tonalite of Fig. 6b). A locality in upper Val Codera (sample location 92-193, indicated in Fig. 7) offers a spectacular and complete transition from magmatic and submagmatic fabrics preserved until a few meters from the contact to particularly intense solid state overprint near the immediate contact. The granodiorite, locally in direct contact with the country rock, is totally transformed into augengneiss. The microstructure of this mylonitic rock reveals ribbons of plastically deformed plagioclase and quartz. Plastically and cataclastically deformed K-feldspar forms augen and extremely elongated lenses. Here, due to strong solid state overprint, the base of the pluton gives the impression of a narrow fault zone, displacing the intrusion in the hangingwall in respect to the country rocks in the footwall. As will be discussed later, the pluton was tectonically emplaced at its base, exposed at the western margin, the foliation development simply being weaker elsewhere because strain was generally accommodated by predominantly magmatic and submagmatic flow.

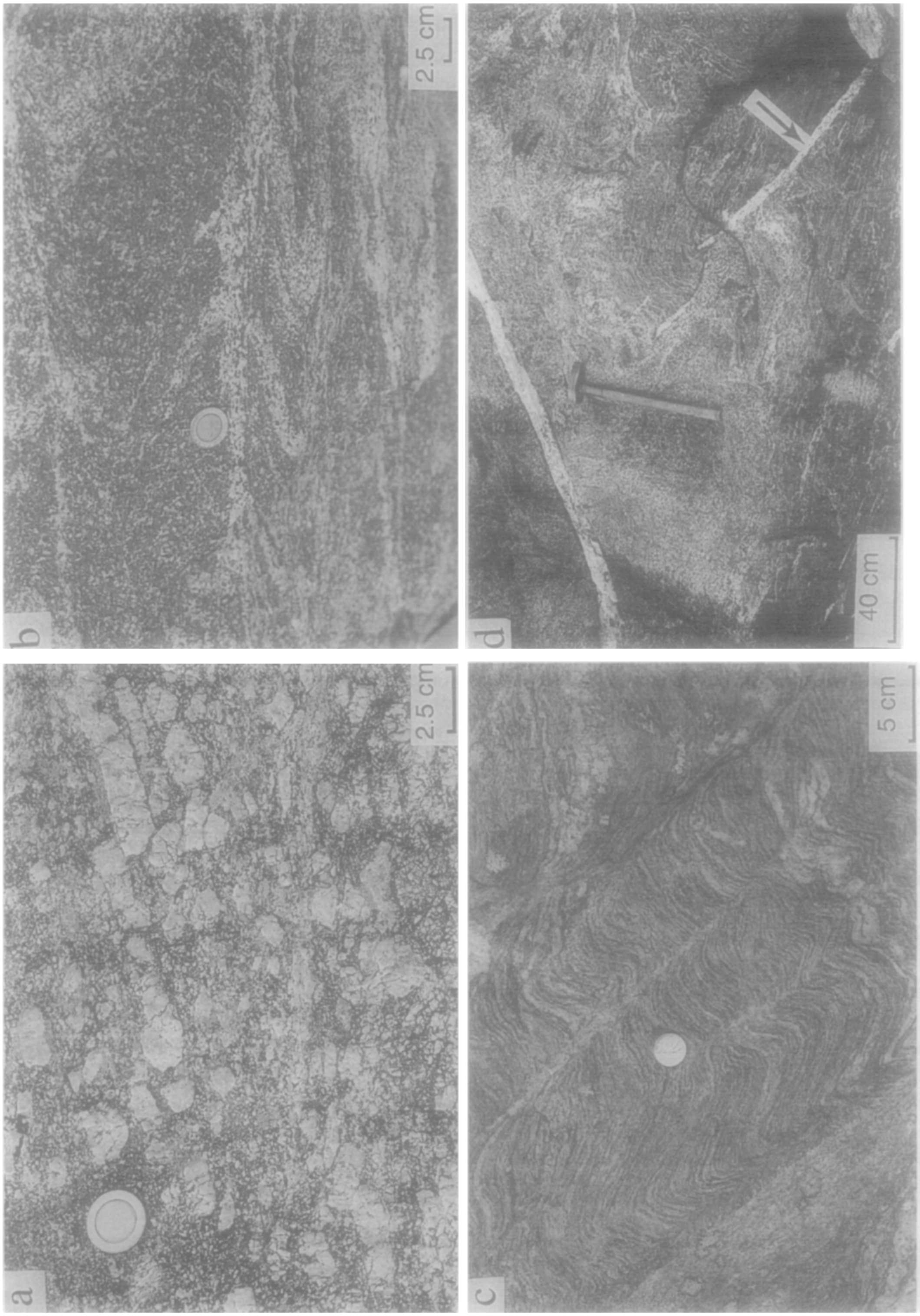
b
2.5 cm
d
40 cm
a
2.5 cm
c
5 cm

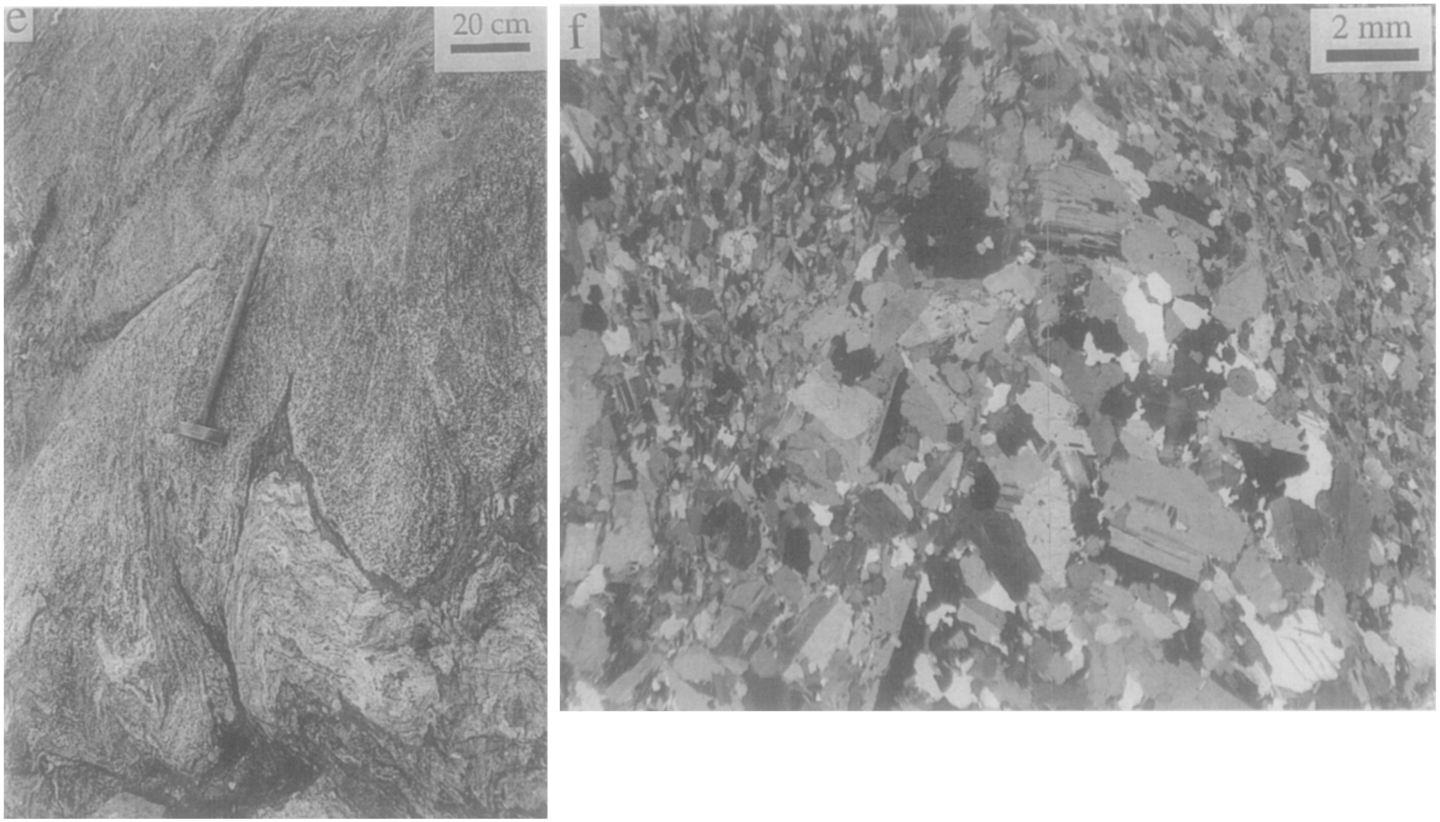

Fig. 5. Fabrics and microstructures from the pluton contact zone in Val Codera (Fig. 5a) and Upper Valle dei Ratti (Fig. 5b–f). (a) Shape fabric of K-feldspar megacrysts in granodiorite from the western contact of the pluton (locality 92-193, see Fig. 7). Tiling of megacrysts indicates dextral shearing (compare Fig. 8). (b) Melt (leucosome) injecting axial planes of small scale folds in tonalite. (c) Melt (leucosome) intruded parallel to axial planes of small scale folds in metapelite from the country rock near the tonalite contact. (d) Mesoscopic shear zone displacing the pluton contact. This shear zone dies out into homogeneous tonalite with a weak magmatic fabric. Note the leucocratic tonalite dike intruded along the shear zone (arrow) and aplite dike cross-cutting the folded tonalite. (e) Mesoscopic folding of the pluton contact between tonalite (top) and country rocks (base). (f) Photomicrograph of a fold in tonalite; the fine-grained part is a folded mafic enclave. Note the folded shape preferred orientation of plagioclase and hornblende without evidence for sub-solidus deformation.

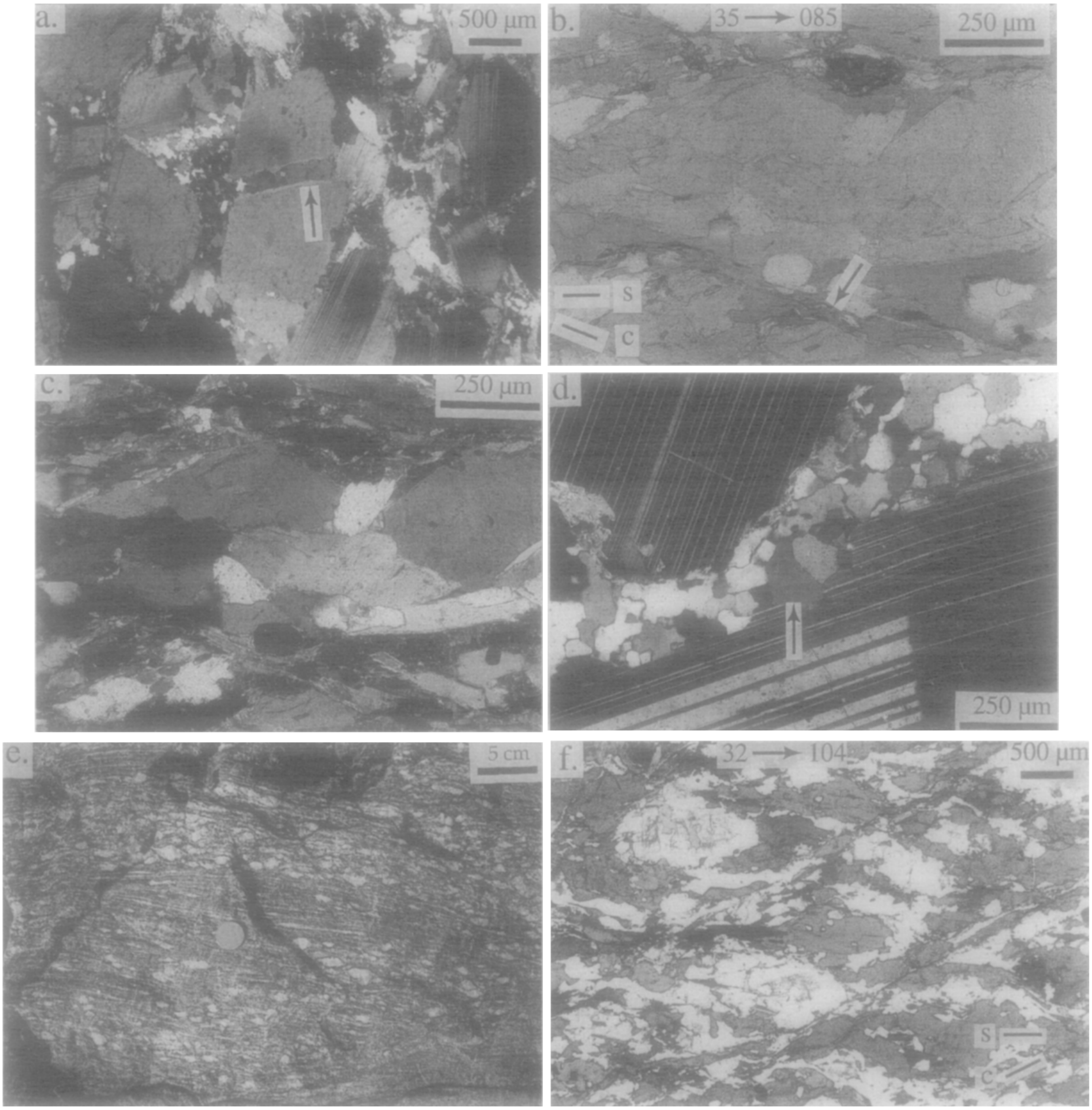

Fig. 6. Submagmatic and solid-state fabrics and microstructures from the western contact. (a) Photomicrograph of a submagmatic fracture in plagioclase (An_{41}) filled with plagioclase (An_{26}) and quartz in granodiorite (locality 92-193, see Fig. 7). The filling plagioclase coats the fracture margin (arrow). Notice the fracture is confined to a single crystal and does not extend through the entire rock. Also note the quartz in the fracture is undeformed while quartz in the matrix is recrystallized. (b) Photomicrograph of deformed hornblende in tonalite from locality 92-130. Shear band (arrow) gives pluton down to the east (sinistral) sense of shear. (c) Same as (b) with analyzer. Note the different optical orientations in the hornblende crystal separated by fractures. This shows that hornblende was deforming mostly by cataclastic flow. (d) Photomicrograph of recrystallized plagioclase (arrow) between plagioclase phenocrysts in granodiorite (locality 92-193). (e) Intensely solid-state deformed granodiorite from contact with country rocks (locality 92-193). White augen are deformed K-feldspar megacrysts. (f) Photomicrograph of S–C fabric in tonalite from near locality 92-89. S–C fabric gives pluton up to the west (dextral) sense of shear.

4.2. Shortening of the contact by synmagmatic folding and thrusting

Map-scale folding of the western contact of the Bergell pluton described earlier is also observed at the scale of the outcrop. The foliation in the tonalite, parallel to the foliation of the underlying country rocks, is folded with fold axial planes roughly parallel to those of the map-scale folds. In the upper Valle dei Ratti the tonalite typically preserved a magmatic foliation, although tightly folded (Fig. 5e). It is clear from regional mapping that this particular fold represents a parasitic fold on the large-scale Valle dei Ratti antiform (Fig. 3b). Hence folding of the Valle dei Ratti antiform, and all the other large-scale antiforms at the base of the pluton, is essentially synmagmatic.

Many microscopic (Fig. 5f) and mesoscopic (Fig. 5b–e) observations confirm that folding of the country rocks and pluton contact occurred while the pluton was still partially molten. An axial planar foliation is generally absent, but a leucocratic melt of tonalitic composition intrudes parallel to the axial planes (Fig. 5b). Similarly, leucosomes intrude parallel to axial planes (Fig. 5c) in tightly folded migmatites of the country rocks near the contact, showing that they were also partially molten. At this contact we also observe boudinaged calc-silicate layers enclosed in the tonalite, with no evidence for sub-solidus deformation in the tonalite. A small-scale shear zone in upper Valle dei Ratti (Fig. 5d) offsets the folded contact and then dies out into apparently undeformed tonalite, and is intruded by leucocratic tonalite. The later aplite and pegmatite dikes, related to the pluton, show that melt was locally present even after folding (Fig. 5d).

The small-scale shear zone depicted in Fig. 5d resembles the southeast dipping thrust of map-scale dimensions described earlier (Fig. 3b). Stretching lineations in the shear zone, accommodating movement along this large thrust, are down dip, sense of shear is top to the north. Shearing of the contact probably occurred at the same time or shortly after folding of the contact because displacement on the shear zone is consistent with N–S shortening indicated by the near vertical E–W striking axial planes of the folds. Evidence for synmagmatic thrusting is found near the tip of this thrust, where it cuts through the tonalite in the hinge zone of the Valle dei Ratti antiform (Fig. 3b). Here, part of this thrusting is accommodated by small-scale shear zones in the tonalite which are synkinematically intruded by granodiorite.

5. Sense of shear determinations and quantitative fabric analysis

As previously discussed, the stretching and mineral lineations in the country rocks and Bergell pluton plunge consistently to the east (Fig. 2). In the Gruf complex, this stretch not only affects the contact to the pluton, but the entire unit. However, unambiguous and consistent sense of shear indicators such as asymmetric porphyroclasts, shear bands and crystal tiling are rarely present. In Val Bondasca asymmetric porphyroclasts and shear bands in country rocks and solid-state deformed tonalite give the same "pluton down-to-the-east" sense of shear (Fig. 6b and 7). By contrast, in the southern part of Val Codera, shear band orientations in solid-state deformed tonalite from the immediate contact give pluton up-to-the-west sense of shear (Fig. 6f). In an outcrop in upper Val Codera (near locality 92-193, see Fig. 7), shear bands give opposite shear senses in the solid state deformed granodiorite and tonalite, while tiling of K-feldspar megacrysts indicates consistent pluton down to the east sense of shear during the magmatic and submagmatic stage. In Valle dei Ratti where foliations and contacts are nearly vertical, senses of shear are consistently dextral.

5.1. The autocorrelation function (ACF)

The autocorrelation function (ACF) is a rapid method for obtaining quantitative shape information (Panozzo-Heilbronner, 1992). In general, ACF's give information on domain size and geometry of domain shapes (e.g., grains); therefore, shape preferred orientations become readily visible. They also allow comparisons of the relative intensity of the fabrics (amount of shape preferred orientation) and grain sizes among samples.

ACF's from 18 samples from the western contact are shown in Fig. 7. Most samples analysed are tonalite with magmatic to submagmatic fabrics. Thin sections were prepared perpendicular to foliation and parallel to the stretching lineation. Images of entire thin sections were ported to a Macintosh, and ACF's were calculated for each of the samples using the public domain software Image 1.28 (Rasband and Reeves, 1990). In Fig. 7, the ACF's are oriented with top (pluton) up and the lineation plunging to the right. Because the images were captured without polarization, the ACF is sensitive to grain shapes between light and dark phases. Eight contour levels (8 levels of grey) are shown for each ACF (see Appendix A). The contours correspond to different size domains in the image, so that the outer contours (lighter shades of grey) correspond to the largest domains. A domain may consist of a group of dark coloured phases, or a single dark crystal surrounded by light phases, or vice versa. Therefore, only the smaller contours reflect the grain sizes. Grain sizes between samples were compared by choosing a suitable contour (in this case contour 96; see Appendix

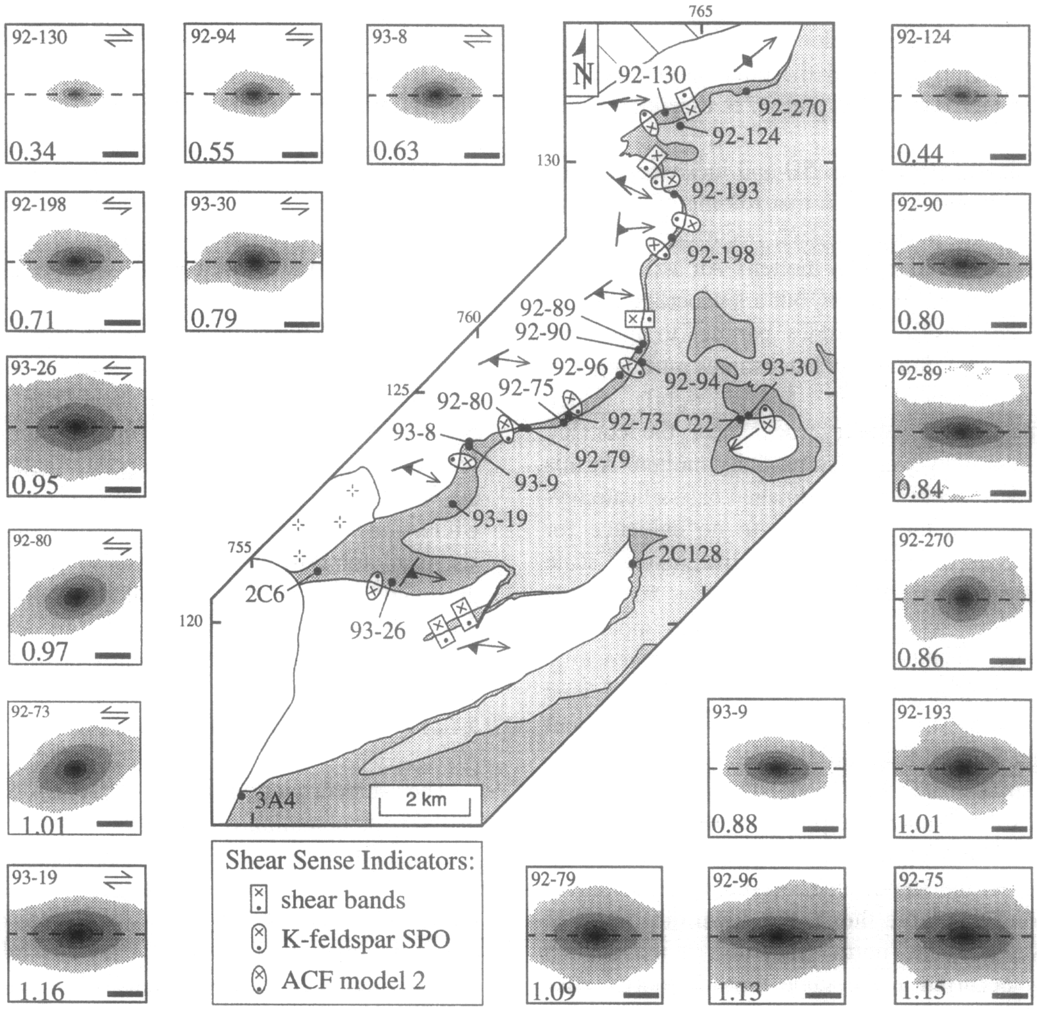

Fig. 7. Map of the western contact showing sample locations and ACF's. Asymmetric ACF's are plotted to the left of the map with top up and lineation plunging to the right (east). ACF grain sizes (mm) are shown in the lower left corner and shear senses in the upper right corner of the ACF's. Scale bars are 1 mm. The macroscopic foliation direction is shown as a dashed line. Shear senses indicated on the map are derived from various indicators shown at their approximate locations: dots indicate movement out of the paper in the direction of the local lineation (shown as arrows with the local foliation). Hornblende geobarometry sample locations (Fig. 9, Table 1) are also shown.

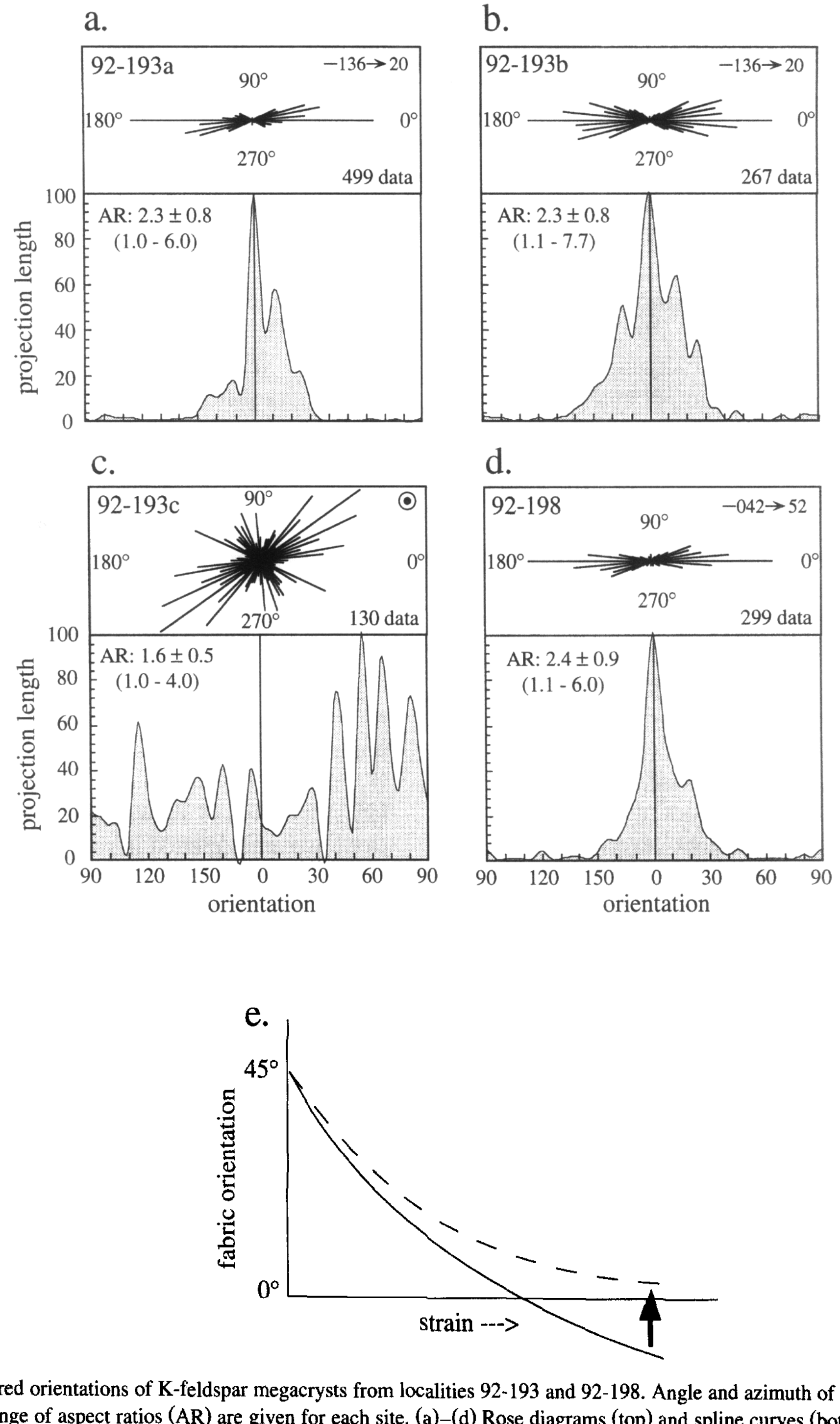

Fig. 8. Shape preferred orientations of K-feldspar megacrysts from localities 92-193 and 92-198. Angle and azimuth of lineation plunge, and average (1σ) and range of aspect ratios (AR) are given for each site. (a)–(d) Rose diagrams (top) and spline curves (bottom) calculated at 5° increments. In (a), (b) and (d), lineation plunges to the right (east) and top is up (90°). The 0° orientation corresponds to the long axis of the enclaves. In (c) the lineation is normal to the page and plunges toward the reader. No foliation is visible, 0° points to the NE. Average aspect ratios (AR) of the megacrysts and range (in parantheses) are given in the upper left of the spline curves. (e) Schematic diagram of fabric orientation vs. strain for rigid particles without interactions (dashed line), modified from Ildefonse et al. (1992a,b). Fabric orientation is approximately equal to the average orientation of the long particles.

A and Panozzo-Heilbronner, 1992), calculating the size of that contour by fitting an ellipse to the contour, and taking the square root of the major axis times the minor axis of the ellipse. Grain sizes calculated in this manner are shown in the lower left-hand corner of the ACF's in Fig. 7. There is a good correspondence between calculated grain size and observed amount of subsolidus deformation for all samples analysed.

The shape of the contours reflects the intensity of a fabric (Panozzo-Heilbronner, 1992), highly elongate contours reflecting good alignments at a given domain scale. Most of the samples in this study have a weak fabric, indicated by elongated contours with small aspect ratios (Fig. 7). The shapes and sizes of the ACF's in Fig. 7 give quick quantitative information on the spatial distribution of relative amounts of preferred orientation and, indirectly, the amount of subsolidus deformation along the western contact.

One way to obtain information on the overall symmetry of a grain shape fabric is to look at the shape of a single contour (Panozzo-Heilbronner, 1992). Because most of the single contour shapes in this study have nearly elliptical contours, no systematic asymmetry could be extracted. We therefore used asymmetries arising from the orientation of long axes of different contour levels for inferring asymmetry. A fabric is defined to be symmetric if the angle between the major axes of contours 128 and 64 (see Appendix A and Panozzo-Heilbronner, 1992) is less than 2 degrees. Such asymmetries indicate that correlation directions change as the domain size changes. Note that this criterion is independent of the orientation of the macroscopically visible foliation trace (dashed line in Fig. 7).

Translating these asymmetries into physical meaning (sense of shear) depends on the knowledge of the exact nature of the fabric elements responsible for the asymmetry. Two alternative models are possible (see Appendix A). Model 1 assumes that the preferred orientation of small domain sizes is deflected from that of the large domains sizes in a sense which corresponds to the sense of the imposed shear, while model 2 assumes the opposite. Taking a classical S–C-fabric as an example, model 1 would predict that the alignment of the smallest domain sizes reflects the C-planes, while that of the largest domains reflects the S-planes. Because the sense of shear, and hence the nature of the shear sense indicator, is unknown in the specimens analysed, the choice of model 2 for inferring sense of shear (half arrows in the upper right-hand corner of the ACF's in Fig. 7) is empirical. This model was chosen because it yields senses of shear consistent with those inferred from traditional criteria in most localities were such criteria were available.

5.2. *Shape preferred orientation (SPO)*

Image analysis is also applied to megacryst-bearing granodiorites (Fig. 5a). Deformed mafic enclaves have X/Z strain ratios around 10. Because of the large strain, we assume that the flattening plane is oriented sub-parallel to the shear zone boundary (in case of a component of simple shear). An asymmetry between the foliation marked by enclaves and shape-preferred orientation of megacrysts is noted by first inspection in many of the outcrops. The outlines of the megacrysts were digitized from field photographs. The orientation of the long axis and aspect ratio of the megacrysts was determined using the program SPAROR, an adapted version of PAROR (Panozzo, 1983) designed for lath shaped (rectangular) shapes. Fig. 8 shows the orientations of feldspars from two areas plotted in rose diagrams and as spline curves enhancing visualization of the data. At site 92-193 (Fig. 8a–c), where granodiorite is in direct contact with the country rocks, analysis was performed in an area dominated by magmatic and submagmatic fabrics. Fig. 8d is from site 92-198 nearby.

The shape preferred orientation of the K-feldspar megacrysts is well developed in sections parallel to the the lineation (Fig. 8a, b, d), and relatively weak perpendicular to lineation (Fig. 8c). Also note that the aspect ratios of the feldspars observed in a section parallel to the lineation are larger. Parallel to the lineation, the largest proportion of the feldspars have their long axes parallel to the trace of the foliation, but a weak asymmetry exists between the foliation trace and the preferred long axis direction of feldspars, with long axes preferring orientations between 0 and 30° (Fig. 8a, b and d).

The development of shape fabrics resulting from the rotation of rigid particles in a viscous matrix has been discussed extensively in the literature (e.g., Ghosh and Ramberg, 1976; Fernandez, 1987; Ildefonse et al., 1992a and references therein). Ghosh and Ramberg (1976) analysed the change in orientation of rigid elliptical particles during combined pure and simple shear. However, their solution does not take into account mechanical interaction between particles. In our example, such interactions evidently played an important role, touching and tiling of megacrysts being very common. Ildefonse et al. (1992a,b) showed that interactions between particles act to slow particle rotations down and concluded that the majority of long axes of particles rotate toward the shear plane with increasing strain during simple shearing, never crossing it (Fig. 8e). Therefore, given possible interactions and simple shearing, all particle axes are expected to lie between 45° and the shear plane (0°).

In our examples (from planes parallel to the lineation), we see that there is a consistent asymmetry between the foliation (assumed to be roughly parallel to the shear plane) and the SPO of the feldspars. From this we conclude that the SPO in the granodiorite formed during top (pluton) down-to-the-east shearing. However, departure from simple shear is very likely, given the weak asymmetry of departures from parallelism with the foliation (indicating a pure shear component if particles interact).

5.3. Comparison of sense of shear indicators

Sense of shear determined from different criteria along the western contact are plotted in their approximate locations in Fig. 7. Since all the ACF samples come from at or near (tens of meters) the contact between tonalite and the country rocks (except sample 92-94), shear senses inferred from these samples give relative displacements between the pluton and the country rocks. The two SPO sites (92-193, 92-198) record senses of shear related to magmatic and submagmatic flow, while the shear band locations 92-130, 92-193 and in Valle dei Ratti formed during solid state flow in tonalite and/or granodiorite. The shear band location north of 92-89 is from tonalite which essentially has a submagmatic fabric. Asymmetries in the ACF mostly relate to magmatic and submagmatic flow.

From Fig. 7, it is evident that the sense of shear was different at different locations along the tonalite/country rock contact. Even the most unambiguous indicators (shear bands) give both pluton up to the west and pluton down-to-the-east senses of shear. However, down-to-the-east movement of the pluton strongly dominates in the northern part of the contact (at and north of locality 92-193) in respect to all stages of deformation (magmatic to solid state). Further south, pluton to-the west movement predominates over a certain distance, and then is reversed yet again. In Valle dei Ratti, a tight synform of tonalite is overprinted by shear band orientations on both limbs of the synform giving dextral senses of shear (the contact being vertical).

In summary, the deduced senses of shear conflict across the entire area of the western contact, and also at particular localities (e.g., shear bands at location 92-193). Therefore, we conclude that deformation at the contact was predominantly accomplished by pure shear associated with E–W extension during that part of the deformation which led to the recorded asymmetries. In fact, the geometry of the large-scale folding of the contact during a late stage in the deformation (that is, after the contact formed) is compatible with overall N–S-shortening and E–W-extension. Also, this same late stage deformation affects the entire Gruf complex and is not restricted to the contact zone of the pluton. The shear bands in the tight syncline of tonalite in Valle dei Ratti indicate very late stage dextral shearing, even post-dating formation of this syncline.

6. Hornblende geobarometry

In order to constrain depths of crystallization of the pluton the Al-in-hornblende geobarometer of Hammerstrom and Zen (1986) was applied to 17 samples from all around the pluton, including the tonalite tail (Table 1, Fig. 9). Sample 2A110 from the eastern contact is a hornblende-bearing granodiorite, all other samples are tonalite. Samples have been collected from near the contact with the country rocks, except for sample 92-270, collected at the immediate contact to the granodiorite core of the pluton. All samples reported in Table 1 have the required nine-phases-assemblage needed to use the barometer (Hammerstrom and Zen, 1986). Hornblende chemistry was measured on the JOEL 8600 superprobe at Basel University, using an accelerating

Table 1
Representative hornblende rim compositions and locations of samples used for the Al-in-hornblende barometry

Sample:	2C25	2C154	2C109	3A4	2C6	93-26	93-19	92-79	A59	92-73	2C128	92-193	C22	92-270	2A91	2A110	A150
SiO_2	42.89	42.20	41.45	42.22	44.14	42.96	42.41	43.47	42.40	43.36	42.67	43.30	42.51	45.39	42.17	44.62	43.92
Al_2O_3	13.88	14.07	12.93	12.55	11.48	10.89	11.52	11.05	12.36	11.95	11.22	10.99	11.59	9.42	11.53	8.71	10.26
TiO_2	0.89	0.92	0.77	0.80	0.73	1.22	0.39	0.96	0.78	0.63	0.87	0.75	0.87	1.01	0.77	0.85	1.07
Fe_2O_3	16.78	17.84	17.67	17.34	16.95	17.58	18.74	17.48	17.92	17.98	17.01	18.33	19.24	15.68	18.48	18.96	18.76
MgO	9.45	9.35	9.36	9.59	10.18	10.04	9.37	10.13	9.48	9.68	9.67	9.77	9.41	11.66	9.69	10.52	10.39
MnO	0.45	0.34	0.46	0.38	0.49	0.42	0.42	0.43	0.46	0.42	0.41	0.39	0.37	0.29	0.46	0.68	0.28
CaO	11.53	11.17	11.65	11.63	11.73	11.65	11.91	12.14	11.80	11.58	12.06	11.95	11.65	11.96	11.89	11.63	11.73
K_2O	0.93	0.98	1.35	1.52	0.88	1.25	1.10	1.20	1.08	0.93	1.32	0.98	1.19	0.98	1.30	0.97	1.10
Na_2O	1.27	1.34	1.13	1.15	1.19	0.98	1.16	1.07	1.27	1.33	1.03	0.97	1.19	0.90	1.22	1.47	1.15
Total:	98.07	98.21	96.75	97.18	97.77	96.99	97.02	97.93	97.55	97.86	96.26	97.43	98.02	97.29	97.51	98.41	98.66
Cations based on 23 oxygens and $Fe^{3+}/(Fe^{3+}+Fe^{2+}) = 0.3$																	
Si	6.306	6.225	6.245	6.319	6.514	6.439	6.388	6.450	6.327	6.428	6.441	6.465	6.347	6.693	6.330	6.625	6.486
(iv)	1.694	1.775	1.755	1.681	1.486	1.561	1.612	1.550	1.673	1.572	1.559	1.535	1.653	1.307	1.670	1.375	1.514
Al (vi)	0.711	0.670	0.541	0.533	0.511	0.362	0.433	0.383	0.500	0.515	0.437	0.399	0.386	0.344	0.369	0.149	0.272
Ti	0.098	0.102	0.087	0.090	0.081	0.137	0.044	0.107	0.088	0.070	0.099	0.084	0.098	0.100	0.087	0.095	0.119
Fe^{2+}	1.444	1.540	1.558	1.519	1.464	1.542	1.652	1.518	1.565	1.560	1.503	1.602	1.681	1.331	1.624	1.648	1.622
Fe^{3+}	0.619	0.660	0.668	0.651	0.628	0.661	0.708	0.651	0.671	0.669	0.644	0.687	0.721	0.570	0.696	0.706	0.695
Mg	2.071	2.056	2.098	2.104	2.240	2.243	2.104	2.241	2.109	2.139	2.176	2.175	2.094	2.568	2.168	2.329	2.288
Mn	0.056	0.042	0.059	0.048	0.061	0.053	0.054	0.054	0.058	0.053	0.052	0.049	0.047	0.042	0.058	0.086	0.035
Ca	1.816	1.765	1.880	1.865	1.855	1.871	1.922	1.930	1.886	1.839	1.950	1.911	1.863	1.873	1.912	1.850	1.856
K	0.174	0.184	0.259	0.290	0.166	0.239	0.211	0.227	0.206	0.176	0.254	0.187	0.227	0.199	0.249	0.184	0.207
Na	0.362	0.383	0.330	0.334	0.340	0.285	0.339	0.308	0.367	0.382	0.301	0.281	0.344	0.338	0.355	0.423	0.329
Total:	15.352	15.404	15.481	15.470	15.346	15.394	15.467	15.419	15.450	15.403	15.418	15.374	15.461	15.365	15.518	15.469	15.423
P(kbar):	8.4	8.6	7.9	7.4	6.5	6.1	6.6	6.2	7.3	6.9	6.5	6.2	6.7	4.8	6.6	4.3	5.6
$\pm 1\sigma$	0.2	0.3	0.3	0.3	0.3	0.7	0.4	0.5	0.5	0.3	0.1	0.5	0.4	0.6	0.4	0.2	0.8
n	18	15	16	12	12	12	16	15	16	15	5	15	16	15	13	6	11
x:	726.15	727.20	735.15	754.75	756.44	758.09	759.44	761.09	761.40	762.03	763.42	764.37	765.60	765.98	774.00	776.08	776.80
y:	115.20	115.30	115.68	116.25	121.09	120.87	122.58	124.22	115.00	124.51	121.29	129.29	124.00	131.53	122.45	133.55	124.65
Elevation:	1040	1260	2080	200	490	935	1630	2035	1100	1880	2640	2620	1400	1570	2080	2770	2570
P^*(kbar):	8.1	8.4	7.9	6.9	6.1	5.8	6.5	6.2	7.1	6.9	6.7	6.4	6.6	4.7	6.6	4.5	5.8

Average pressures (P) calculated using Al-in-hornblende barometer of Schmidt (1992) for n rim compositions; normalization scheme is the same as used by Schmidt (1992) (see text). x, y are Swiss geographical coordinates. Elevation is in meters. P^* is pressure normalized for an elevation of 2000 m (used in Fig. 9).

voltage of 15 kV, a beam current of 10 μA and a beam diameter of about 3 μm. All elements were measured by WDS with counting times between 10 and 20 s. Natural and synthetic standards were used and the data were reduced using ZAF.

Following Leake (1978), most of the amphiboles measured in this study range from edenitic hornblende to magnesian hastingsitic hornblende (Table 1). $Mg/(Mg + Fe^{2+})$ ranges from 0.55 to 0.71, and Na + K from 0.47 to 0.62. In all samples hornblende is zoned with an increase in total Al and a slight decrease in $Mg/(Mg + Fe^{2+})$ toward the rim. A minimum of 5, but typically 15 rim analyses were used to calculate the average pressure for a given sample (Table 1). Pressures were calculated using the experimental calibration of Schmidt (1992). Following Schmidt (1992), we normalized hornblende compositions based on: (1) 23 oxygens and assuming $Fe^{3+}/(Fe^{3+} + Fe^{2+}) = 0.3$, and (2) Σ cations–Ca–Na–K = 13. Compositions were considered valid only when both normalization schemes gave similar formulas. Reported errors are standard deviation of the mean ($\pm 1\sigma$), and do not include analytical or calibration uncertainties. Schmidt (1992) quotes an uncertainty of ±0.6 kbar for his calibration. Calculated pressures, normalized to an elevation of 2000 m (P^* in Table 1), range from 4.3 ± 0.2 to 8.6 ± 0.3 kbar (Table 1).

Fig. 9 also reports the pressures obtained by Reusser (1987) who used the Al-in-hornblende barometer of Hollister et al. (1987). These data have been recalculated using the barometer of Schmidt (1992) and also normalized to an elevation of 2000 m. These data are merely shown for comparison in Fig. 9 and have not been used for contouring because of some incompatibilities with our data set. Particularly, at one locality in Val Mera, Reusser (1987) obtained much lower pressures ($P^* = 6.1$ kbar vs. $P^* = 6.9$ kbar, Fig. 9). We attribute the lower pressures given by Reusser (1987) to problems arising from the strong solid state overprint in many tonalites. This overprint may lead to re-equilibration in the hornblende rim below the solidus. Additionally, we found cataclastic fragmentation of hornblende to be very common, so that many "rims" are actually cleaved portions of the core of the once larger hornblende. Hornblende cores have relatively low Al-content and probably crystallized early. Therefore, the Al content of hornblende cores are not buffered by the required 9 phase assemblage, and are not dependent on pressure. Regarding our own data, we took care to avoid measurements in specimens with a strong solid-state overprint.

In Fig. 9 the tonalite tail is restored to its approximate geometry by retrodeformation of movements along the southeast striking Riedel shears present

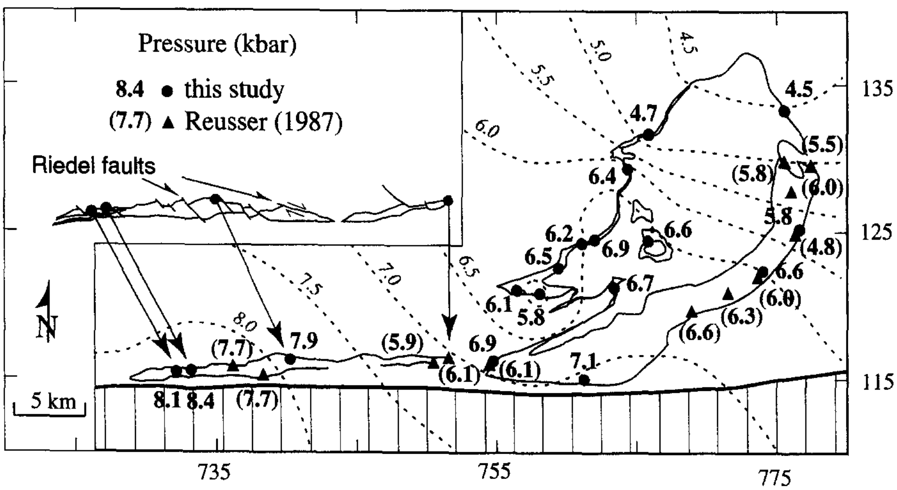

Fig. 9. Map of crystallization pressures (in kbar) from the Bergell pluton determined from the Al-in-hornblende geobarometer. Pressures are normalized to 2000 m (P^*, see text). See Table 1 and Figs. 7 and 9 for sample numbers and exact locations. Contours (white dashed lines) are based on data from this study (Table 1). The data from Reusser (1987) are shown in parenthesis for comparison. The tonalite tail is restored to its approximate shape at the time of crystallization. The present day geometry of the tonalite tail is also shown, with sample locations before and after restoration connected by arrows.

along the tail. This faulting post-dates crystallization of the tail and is related to late stage brittle dextral strike slip along the Insubric fault (Fumasoli, 1974). It amounts to 30% extension of the tail west of Val Mera.

6.1. Discussion of the hornblende geobarometry

There are no systematic differences in pressure determined from the Al-in-hornblende geobarometry from Valle dei Ratti to upper Val Codera, suggesting that this part of the pluton intruded and cooled through its solidus at about the same depth of 22–26 km (6–7 kbar). This is consistent with the interpretation that this part of the pluton (the western contact) represents the exposed floor of the Bergell pluton.

Over the entire area of Fig. 9, pressures increase from northeast to southwest, the strike of the contours being ill-constrained in the region of the tonalite tail. The E–W gradient may be interpreted to be caused by differential exhumation due to tilting after solidification of the pluton, as already noted by Reusser (1987). Since uplift and exhumation of the entire Lepontine dome, including the Begell pluton, are intimately related to backthrusting along the Insubric mylonite belt, the amount of backthrusting decreasing from west to east (Schmid et al., 1989), the choice of a N–S axis of tilting, i.e. at a right angle to the Insubric line delimiting the Lepontine area from the unmetamorphic Southern Alps, is appropriate on structural grounds. The tilt angle derived from such a simple model amounts to between 7° and 11° along E–W-traverses through the tonalite tail, and through the central part of the main pluton, respectively (see discussion by Rosenberg and Heller, in prep.). Note however, that the total amount of tilting inferred from geobarometry is most likely to be underestimated because it only records that part of the exhumation history which occurred after the solidus was reached. In fact, structural arguments (Rosenberg et al., 1995; Berger and Gieré, 1995) point to a total tilt angle of about 20°, exposing a 10 km thick interval in terms of crustal depth along an E–W-section across the pluton.

The north–south component of the pressure gradient is only reliably constrained in the northeastern corner of the intrusion (Fig. 9). Note however, that the hornblende-bearing granodiorite (sample 2A110; $P^* = 4.5$ kbar, Fig. 9) has a lower solidus temperature than tonalite, and therefore the calibration of Schmidt (1992) may not apply. Tonalite sample 92-270 ($P^* = 4.7$ kbar, Fig. 9), on the other hand, comes from the immediate contact with the granodiorite, and therefore, may have completely crystallized after the rest of the analysed tonalites (which come from near the contact with the country rocks), and after a significant amount of erosion had occurred. Taking the difference in pressure between sample 92-270 (4.7 kbar) and sample 92-193 (6.4 kbar, Fig. 9) at the western margin an apparent vertical distance of 6.3 km would be deduced if both samples had cooled through the solidus contemporaneously. However, the horizontal separation of these samples is only 2.75 km. Taking a reasonably fast denudation rate of 5 km/Ma (Giger and Hurford, 1989) at the time of intrusion, specimen 92-270 ($P^* = 4.7$ kbar) would have crossed the solidus about 1 Ma after 92-193 ($P^* = 6.4$ kbar). This is a reasonable length of time for melt to be present in the deep crust, given the fact that the initial temperature of the country rocks was high at the time of intrusion (Davidson et al., 1994). Independently, geochronological evidence (von Blanckenburg, 1992) indicates that the granodiorite crystallized about 2 Ma after the tonalite at the eastern margin of the pluton.

In summary, geobarometry indicates that synmagmatic folding at the western contact took place at considerable depth (at least 22–26 km). It also provides independent evidence for large-scale tilting due to differential exhumation of the Bergell pluton postulated on structural grounds. However, amount and rotation axis of post-solidifation tilting are ill-constrained by these data, because it cannot be assumed that the solidus was reached contemporaneously over the entire area of the pluton (see Berger et al., 1996).

7. Discussion

7.1. Geometry of the pluton

Contour maps (Fig. 4) and cross sections (Fig. 3) show that the base of the cenral part of the Bergell pluton overlies the country rocks along its present-day western margin (Fig. 1). The tonalite tail roots in the

Southern Steep Belt north of the Insubric mylonites. Indeed, as already suggested by Wenk (1973), the Bergell pluton has the geometry of a nappe. This nappe-like geometry is reinforced by the observation that discontinuous layers of ultramafic, mafic and calc-silicate rocks can be followed all along the base of the pluton (black layer in Fig. 3a). This leads to the postulate that the pluton was intruded and/or emplaced along a former nappe boundary (Diethelm, 1989), corresponding to the North-Penninic suture zone (Schmid et al., 1996), i.e. the Misox zone between the Adula and Tambo nappes (Fig. 1a). Hornblende geobarometry indicates that the tonalites at the base of the pluton crystallized at approximately constant depth (6–7 kbar) along a large portion of the folded western contact (Fig. 9), which therefore had to be flat-lying at the time the tonalites reached the solidus. In profile view (Fig. 3a), the pluton occupies the same structural position as the Tambo and Suretta nappes north of the Engadine line, i.e. between the Adula–Gruf unit at the base and the South-Penninic Malenco–Lizun ophiolite complex on top (Fig. 3a), dissected by the post-magmatic Engadine line (Schmid and Froitzheim, 1993).

Small remnants of the Tambo and Suretta nappes are present south of the Engadine line but discordantly cut by the granodiorite (to the right of the word "Lizun" in Fig. 3a) which has a younger crystallization age with respect to the tonalite near the eastern margin of the Bergell pluton (but not at its base in the west!), based on both structural (Berger and Gieré, 1995) and geochronological (von Blanckenburg, 1992) arguments. As discussed by Rosenberg et al. (1995) and Berger and Gieré (1995) the eastern contact is interpreted to represent the side of the pluton near its roof (compare Figs. 1 and 3a). The structural features at the eastern margin indicate ballooning (Conforto-Galli et al., 1988), related to the final stages of pluton emplacement at a very much higher structural level (corresponding to less than 5 kbar according to hornblende barometry).

The tonalite tail south and west of the main body of the pluton forms a tabular body, interpreted as the feeder to the pluton (Rosenberg et al., 1994, 1995). This study provides the following evidence supporting this interpretation: (1) According to hornblende barometry the tonalite tail crystallized at greater depths than the main body of the pluton; (2) Structurally, the main body of the pluton has the geometry of a nappe that steepens in the south toward the Insubric shear zone, and hence no feeder dyke is expected beneath the main body of the pluton. Interestingly, all Alpine-age mantle-derived plutons (e.g., the Ademello pluton and many small bodies of tonalite) occur in close proximity to the Periadriatic line (i.e. the Insubric line in our area, Schmid et al., 1989). This suggests that these mantle-derived magmas used the Insubric fault zone to gain access to the middle and upper crust.

7.2. The predominance of magmatic and submagmatic flow during regional deformation

Mesoscopic fabrics and microstructures from the igneous rocks found along the base of the pluton exposed at its western contact (Figs. 5 and 6) indicate that final emplacement and cooling of the pluton are intimately related to regional deformation, as previously suggested by Wenk (1973). Most of the deformation experienced by these rocks occurred in the magmatic and submagmatic state. Solid-state deformation is pervasive in a few locations only, and restricted to the immediate contact with the country rocks. If present at other sites, it is concentrated in particular (high-stress) microstructural sites (Fig. 6d).

According to Miller and Paterson (1994) submagmatic fabrics and microstructures in plutons are rare at higher crustal levels because of the transitory nature of the submagmatic stage. Along the western contact of the Bergell pluton, however, submagmatic flow predominates. Together with the high ambient temperatures at great depth (22–26 km) and the large size of the pluton, this indicates that the cooling rate was slow (Miller and Paterson, 1994). Note also, that near the solidus, low melt fractions remain over a larger temperature interval in tonalitic compared to SiO_2-richer magmas (Bouchez et al., 1992).

7.3. Synmagmatic regional deformation

Strictly speaking, two stages of deformation are distinguished along the base of the Bergell pluton. The first stage has produced the ubiquitous well-developed, and locally very strong, planar fabric. During a second stage, this fabric and the contact itself were folded together during N–S shortening. Both deformation stages, however, occurred before complete crystallization of the pluton, and therefore during a relatively short period of time.

We intepret the formation of the foliation to be related to the emplacement of the main part of the pluton over the underlying units. Arguments for tectonically driven emplacement from south to north are the following: (1) the tabular feeder of the pluton is located to the south of the main mass of the pluton and immediately north of, and along, the Insubric mylonite belt (Berger et al., 1996) and (2) the pluton has the geometry of a nappe and occupies the same structural position as the Tambo and Suretta nappes (Fig. 3a). Emplacement of the pluton is interpreted to be part of a regional deformation phase (the Niemet–Beverin phase of Schmid et al., 1996 tentatively dated at 35–30 Ma), accompanied by vertical extrusion in the Southern Steep Belt (Merle, 1994; Berger et al., 1996) and late-stage differential northward displacement of the Tambo and Suretta nappes (see Schmid et al., 1990; Merle and Guillier, 1989). Such a scenario elegantly solves the space problem during pluton emplacement (Fig. 10a).

Evidence for the regional character of the second deformation stage (synmagmatic folding of the foliation) is direct, because folding of the base of the pluton also affects the underlying Adula–Gruf unit (Fig. 10b). According to Rosenberg et al. (1995), folding of the base of the pluton forced magma to higher structural levels, thus causing ballooning near the roof of the pluton (eastern contact). This folding stage is directly linked with the formation of the Cressim antiform (Fig. 1b) and hence to the formation of that part of the Southern Steep Belt (Milnes, 1974; Berger et al., 1996). Therefore, the onset of backfolding in the Bergell Alps predates complete crystallization of the pluton (32–30 Ma according to von Blanckenburg, 1992). This shows that vertical extrusion and backfolding in the Bergell Alps must have initiated much earlier than previously assumed by Hurford et al. (1989) and Schmid et al. (1987). However, as discussed by Berger et al. (1996), backthrusting along the Insubric mylonite belt post-dates the synmagmatic deformation described here.

In spite of the necessity for two deformation stages, the timing relationships between the formation of foliation and lineation at the base of the pluton and folding of the foliated contact zone are

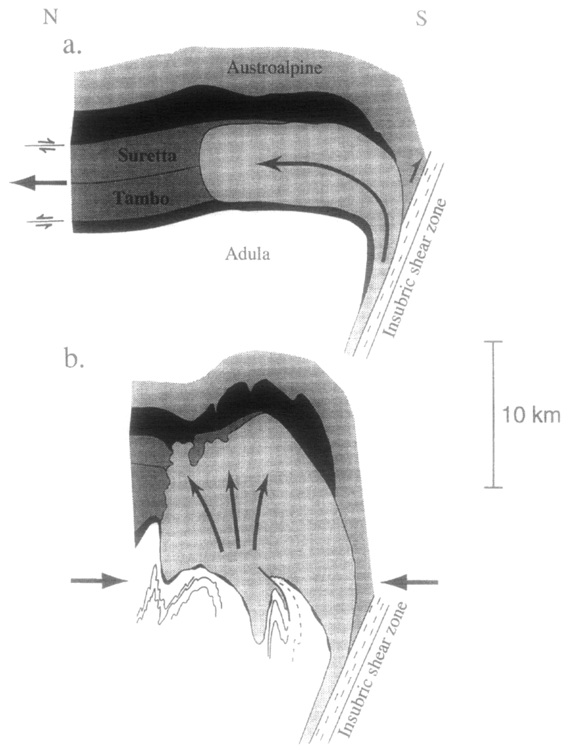

Fig. 10. Schematic cross-sections depicting the intrusion history of the Bergell pluton. (a) The Bergell pluton (light gray) is emplaced as a magma from south to north over the underlying Adula nappe. The well-developed foliation along the base of the pluton probably formed at this time (the first deformation step, see text). The black unit below the pluton and Tambo nappe represents, from north to south: the Misox zone, the Chiavenna ophiolite complex, the band of ultramafic, mafic and calc-silicate rocks present along the base of the Bergell pluton, and finally, the Bellinzona–Dascio zone. The black unit above the pluton and Suretta nappe represents the Lizun and Malenco ophiolite complexes. (b) The base of the Bergell pluton is folded during N–S compression and simultaneous E–W extension while it is still partially molten (the second deformation step, see text). Shortening of the base of the pluton forces remaining magma to intrude the crust at higher structrual levels (arrows), causing flattening of the contact metamorphic aureole near the top of the pluton (eastern contact).

problematic. This is because the E–W lineation and foliation appear to have formed together. On the other hand, the foliation must have formed during the first deformation step and before it was folded during N–S compression and contemporaneous E–W extension (the second deformation stage). Opposing senses of shear at the base of the pluton (Fig. 7) associated with the formation of the lineation suggest that E–W extension was coaxial during the second deformation stage. This stretch was probably coeval with ongoing N–S shortening which eventually lead to folding of the contact. Contemporaneous N–S shortening and E–W extension is in fact compatible with the model proposed by Schmid et al. (1989) for exhumation and east-directed lateral escape of the Central Alps during movements along the Insubric shear zone (see also Schmid and Froitzheim, 1993), and with similar scenarios proposed for other areas (e.g., Mancktelow and Pavlis, 1994). Nowhere could we observe refolding of the E–W lineation contained in the foliation, the E–W fold axes of the regional-scale folds turning ENE–WSW in the east being everywhere parallel to the stretching lineations (compare Figs. 1–3). Most likely, formation of the foliation, subsequent folding and formation of the lineation must have occurred during progressive deformation and do not represent separate events.

Giger and Hurford (1989) show that the Bergell pluton cooled rapidly during and after crystallization and suggest that the entire Central Alps were exhumed as more or less a rigid block due to strain localization within the Insubric mylonite belt during backthrusting. Therefore, backthrusting along the Insubric shear zone and associated tilting of the pluton must have outlasted the synmagmatic deformations.

8. Conclusions

Evidence for predominantly magmatic and submagmatic flow encountered at the base of the pluton show that regional deformation affected the pluton during its final emplacement and while it was cooling. Two stages of synmagmatic deformation are distinguished. The first stage produced a well-developed foliation all along the base of the pluton. This foliation formed during northward emplacement of the pluton over the underlying units while the pluton was still partially molten (Fig. 10a). Shortly after this stage, and before complete crystallization, the foliation at base of the pluton was folded together with the country rocks (the second deformation stage) during N–S shortening and E–W stretching (Fig. 10b). Rapid erosion and subsequent differential motion along the Insubric shear zone, exhumed and tilted the Bergell pluton, offering a unique crustal cross-section through a pluton emplaced and deformed during regional deformation.

These findings lead to the following conclusions which are of general interest: (1) The final emplacement (and probably also the ascent) of this pluton took place in a demonstrably compressive environment (Hollister and Crawford, 1986) related to late stage shortening of the Alpine orogen; (2) this partially molten pluton behaved very much like the underlying country rocks, deformed in the solid-state at high temperatures and deep in the crust; and partially molten plutons are apparently able to transmit stresses from and to their solid-state deformed country rocks during regional deformation at deep crustal levels. Consequently, these country rocks must have deformed at very low differential stresses.

Acknowledgements

Support from the Schweizerische Nationalfonds grants 21-29804.90 and 20-35891.92 is gratefully acknowledged. We thank Alfons Berger, Reto Gieré, Christian Hafner, Renée Panozzo, Niko Froitzheim and Holger Stünitz for their help and discussions during this study. Comments of the two reviewers Jean-Luc Bouchez and Neil Mancktelow improved the content. We also acknowledge having been influenced by the ideas of Linc Hollister which inspired us to have a closer look at the Bergell intrusion.

Appendix A. ACF example

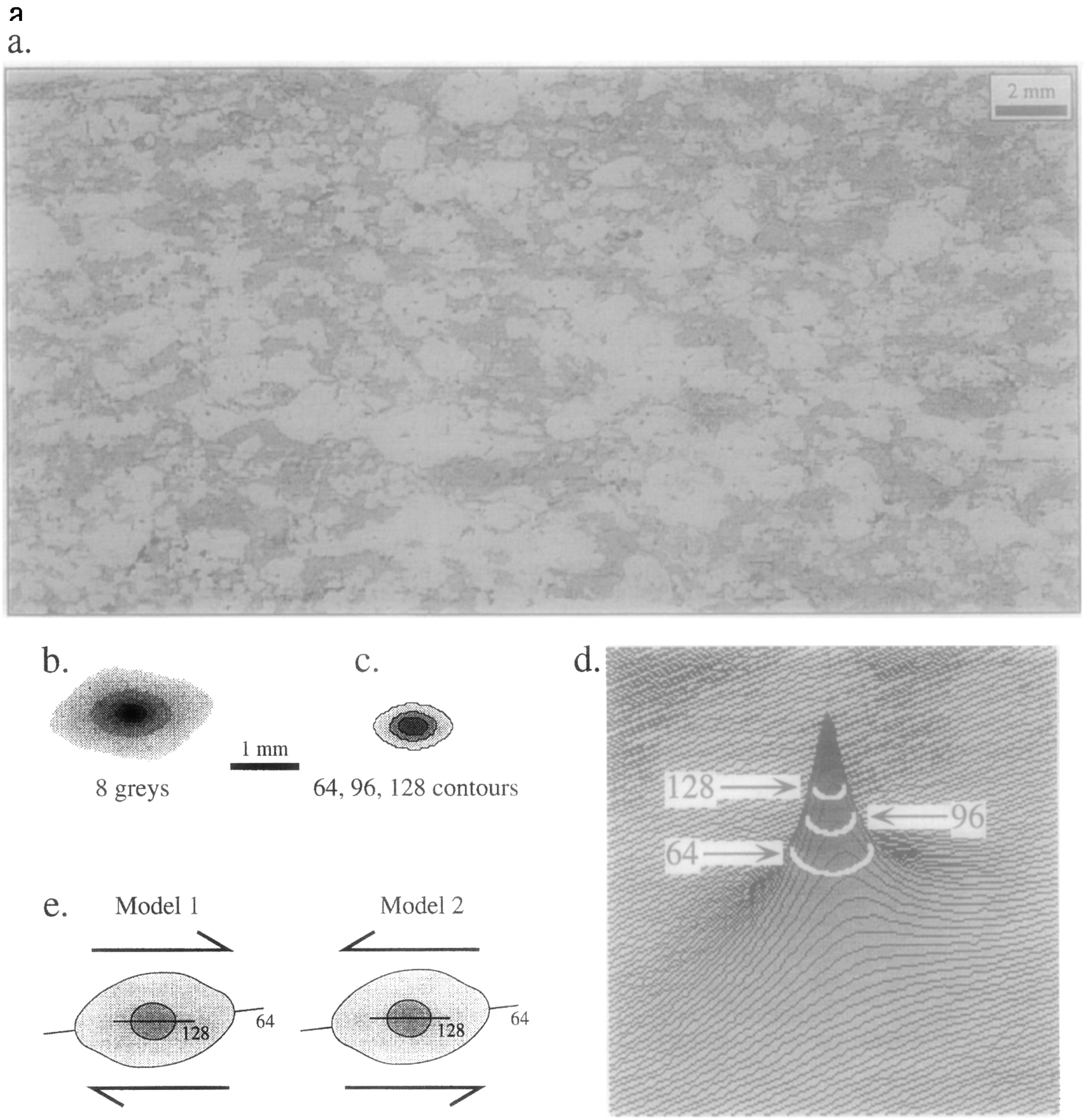

Description: (a) Example of a captured imgae (92-94). (b) Two-dimensional ACF displayed with 8 gray levels (gray values from 1 to 256 and corresponding to different domain sizes. (c) Two-dimensional ACF with the 64 (outside), 96 (middle) and 128 (inside) contours. (d) Three-dimensional ACF showing the approximate locations of the 64 (1/4 peak height), 96 (3/8 peak height) and 128 (1/2 peak height) contours. (e) Sense of shear models (discussed in text).

References

Arzi, A.A., 1978. Critical phenomena in the rheology of partially melted rocks. Tectonophysics, 74: 173-184.

Berger, A. and Gieré, R., 1995. Structural observations at the eastern contact of the Bergell Pluton. Schweiz. Mineral. Petrogr. Mitt., 75: 147-161.

Berger, A., Rosenberg, C. and Schmid, S.M., 1996. Ascent, emplacement and exhumation of the Bergell pluton within to the Southern Steep Belt of the Central Alps. Schweiz. Mineral. Petrogr. Mitt., in press.

von Blanckenburg, F., 1992. Combined high precision chronometry and geochemical tracing using accessory minerals: applied to the Central-Alpine Bergell intrusion. Chem. Geol., 100: 19-40.

von Blanckenburg, F., Früh-Green, G., Diethelm, K. and Stille, P., 1992. Nd-, Sr-, O-Isotopic and chemical evidence for a two stage contamination history of mantle magma in the Central-Alpine Bergell intrusion. Contrib. Mineral. Petrol., 110: 33-45.

Bouchez, J.-L., Delas, C., Gleizes, G., Nédélec, A. and Cuney, M., 1992. Submagmatic microfractures in granites. Geology, 20: 35-38.

Bucher-Nurminen, K. and Droop, G., 1983. The metamorphic evolution of garnet- cordierite-sillimanite gneisses of the Gruf Complex. Contrib. Miner. Petrol., 84: 215-227.

Conforto-Galli, C., Spalla, M., Gosso, G. and Montrasio, A., 1988. Synintrusive foliation of the Masino-Bregaglia tonalite and its roof pendants in Val Sissone (Val Malenco, Central Alps, Italy). Rend. Soc. Ital. Mineral. Petrol., 43: 509-516.

Davidson, C., Schmid, S.M. and Hollister, L.S., 1994. Role of melt during deformation in the deep crust. Terra Nova, 6: 133-142.

Diethelm, K., 1989. Petrographische und Geochemische Untersuchungen an Basischen Gesteinen der Bergeller Intrusion. Ph.D. Diss., ETH-Zürich.

Droop, G.T. and Bucher-Nurminen, K., 1984. Reaction textures and metamorphic evolution of Sapphirine-bearing Granulites from the Gruf Complex, Italian central Alps. J. Petrol., 25: 766-803.

Fernandez, A., 1987. Preferred orientation developed by rigid markers in two-dimensional simple shear strain: a theoretical and experimental study. Tectonophysics, 136: 151-158.

Fumasoli, M.W., 1974. Geologie des Gebietes Nördlich und Südlich der Iorio-Tonale Linie, im Westen von Gravedona (Como, Italia). Ph.D. Diss., ETH-Zürich.

Ghosh, S.K. and Ramberg, H., 1976. Reorientation of inclusions by combination of pure shear and simple shear. Tectonophysics, 34: 1-70.

Giger, M. and Hurford, A.J., 1989. Tertiary intrusives of the Central Alps: Their Tertiary uplift, erosion, redeposition and burial in the South-Alpine foreland. Eclogae Geol. Helv., 82: 857-866.

Guineberteau, B., Bouchez, J-L. and Vigneresse, J.-L., 1987. The Mortagne granite pluton (France) emplaced by pull-apart along a shear zone: Structural and gravimetric arguments and regional implication. Geol. Soc. Am. Bull., 99: 763-770.

Hafner, M., 1993. Strukturgeologische und Geochemische Untersuchungen von Leukokraten Granit-Gängen und Migmatiten der Südlichen Adula am Monte Peschiera (Italia). Diploma Thesis, Univ. Basel.

Hammerstrom, J.M. and Zen, E-an, 1986. Aluminium in hornblende: An empirical igneous geobarometer. Am. Mineral., 71: 1297-1313.

Hänny, R., Grauert, B. and Soptrajanova, G., 1975. Paleozoic migmatites affected by high grade Tertiary metamorphism in the Central Alps (Valle Bodengo, Italy): A geochronological study. Contrib. Mineral. Petrol., 51: 173-196.

Hansmann, W., 1981. Geologisch-Petrographische Untersuchungen im Südlichen Bergell: Val Ligoncio. Diploma Thesis, ETH Zürich.

Heitzmann, P., 1975. Zur Metamorphose und Tektonik im südöstlichen Teil der Lepontinischen Alpen. Schweiz. Mineral. Petrogr. Mitt., 55: 467-522.

Heitzmann, P., 1987. Evidence of late Oligocene/early Miocene backthrusting in the Central Alpine "root zone". Geodinamica Acta, 1: 183-192.

Hollister, L.S. and Crawford, M.A., 1986. Melt-enhanced deformation: a major tectonic process. Geology, 14: 558-561.

Hollister, L.S., Grissom, G.C., Peters, E.K., Stowell, H.H. and Sisson, V., 1987. Confirmation of the empirical correlation of aluminium in hornblende with pressure of solidification of calcalkaline plutons. Am. Mineral., 72: 231-239.

Hunziker, J.C., Desmos, J. and Hurford, A.J., 1992. Thirty Two Years of Geochronological Work in the Central and Western Alps: A Review on Seven Maps. Mém. Géol. (Lausanne), 13, 59 pp.

Hurford, J., 1986. Cooling and uplift patterns in the Lepontine Alps (South Central Switzerland) and an age of vertical movement on the Insubric fault line. Contrib. Mineral. Petrol., 92: 413-429.

Hurford, J., Flisch, M. and Jäger, E., 1989. Unravelling the thermo-tectonic evolution of the Alps: a contribution from fission track analysis and mica dating. In: M. Coward, D. Dietrich and R. Parks (Editors), Alpine Tectonics. Spec. Publ. Geol. Soc. London, 45: 153-171.

Ildefonse, B., Launeau, P., Bouchez, J.L. and Fernandez, A., 1992a. Effect of mechanical interactions on the developement of shape preferred orientation: a two dimensional experimental approach. J. Struct. Geol., 14: 73-84.

Ildefonse, B., Sokoutis, D. and Mancktelow, N.S., 1992b. Mechanical interactions between rigid particles in a deforming ductile matrix. Analogue experiments in simple shear flow. J. Struct. Geol., 14: 1253-1266.

Leake, B.E., 1978. Nomenclature of amphiboles. Mineral. Mag., 42: 533-563.

Mancktelow, N.S. and Pavlis, T.L., 1994. Fold-fault relationships in low-angle detachment systems. Tectonics, 13: 668-685.

Merle, O., 1994. Syn-convergence exhumation of the Central Alps. Geodinamica Acta, 713: 129-138.

Merle, O. and Guillier, B., 1989. The building of the Central Swiss Alps: an experimental approach. Tectonophysics, 165: 41-56.

Merle, O., Cobbold, P. and Schmid, S.M., 1989. Tertiary kinematics in the Lepontine dome. In: M. Coward, D. Dietrich and R. Parks (Editors), Alpine Tectonics. Geol. Soc. Spec. Publ., 45: 153–171.

Miller, R.B. and Paterson, S.R., 1994. The transition from magmatic to high-temperature solid-state deformation: implications from the Mount Stuart batholith, Washington. J. Struct. Geol., 16: 853–865.

Milnes, A.G., 1974. Structure of the Pennine Zone (Central Alps): a new working hypothesis. Geol. Soc. Am. Bull., 85: 1727–1732.

Moticska, P., 1970. Petrographie und Strukturanalyse des westlichen Bergeller Massivs und seines Rahmens. Schweiz. Mineral. Petrogr. Mitt., 50: 355–443.

Panozzo, R., 1983. Two-dimensional analysis of shape fabric using projections of digitized lines in a plane. Tectonophysics, 95: 279–295.

Panozzo-Heilbronner, R., 1992. The auto correlation function: an image processing tool for fabric analysis. Tectonophysics, 212: 351–370.

Paterson, S.R., Vernon, R.H. and Tobisch, O.T., 1989. A review of criteria for the identification of magmatic and tectonic foliations in granitoids. J. Struct. Geol., 11: 349–363.

Rasband, W. and Reeves, A., 1990. Image 1.28. National Institue of Health, Research Services Branch NIMH.

Reusser, E., 1987: Phasenbeziehung im Tonalit der Bergeller Intrusion. Ph.D. Thesis, Min. Inst. ETH Zürich.

Rosenberg, C. and Heller, F., (submitted): Tilting of the Bergell pluton and Central Lepontine area: evidence from paleomagnetic data. Eclogae Geol. Helv.

Rosenberg, C., Berger, A., Davidson, C. and Schmid, S.M., 1994. Emplacement of the Masino-Bregaglia (Bergell) pluton, Central Alps. Atti Ticinensi Sci. Terra, Serie Spec., 1: 31–39.

Rosenberg, C., Berger, A. and Schmid, S.M., 1995. Observations from the floor of a granitoid pluton: Inferences on the driving force of final emplacement. Geology, 23: 443–446.

Schmid, S.M. and Froitzheim, N., 1993. Oblique slip and block rotation along the Engadine line. Eclogae Geol. Helv., 86: 569–594.

Schmid, S.M., Zingg, A. and Handy, M., 1987. The kinematics of movements along the Insubric Line and the emplacement of the Ivrea Zone. Tectonophysics, 135: 47–66.

Schmid, S.M., Aebli, H.R., Heller, F. and Zingg, A., 1989. The role of the Periadriatic Line in the tectonic evolution of the Alps. In: M. Coward, D. Dietrich and R. Parks (Editors), Alpine Tectonics. Spec. Publ. Geol. Soc. London, 45: 153–171.

Schmid, S.M., Rück, P. and Schreurs, G., 1990. The significance of the Schams nappes for the reconstruction of the paleotectonic and orogenic evolution of the Penninic zone along the NFP-20 East traverse (Grisons, eastern Switzerland). Mém. Soc. Géol. Fr., 156: 263–287.

Schmid, S.M., Froitzheim, N., Pfiffner, O.A., Schönborn, G. and Kissling, E., 1996. Geophysical-geological transect and tectonic evolution of the Swiss–Italian Alps. Tectonics, in press.

Schmidt, M., 1992. Amphibole composition in tonalite as a function of pressure: an experimental calibration of the Al-in-hornblende barometer. Contrib. Mineral. Petrol., 110: 304–310.

Schmutz, H., 1976. Der Mafit–Ultramafit-Komplex zwischen Chiavenna und Val Bondasca. Beitr. Geol. Karte Schweiz., N.F. 149, 73 pp.

Spillmann, P., 1993. Die Geologie des Penninisch–Ostalpinen Grenzbereichs im Südlichen Berninagebirge. Ph.D. Thesis, Geol. Inst. ETH Zürich.

Trommsdorff, V. and Evans, B.W., 1972. Progressive metamorphism of antigorite schist in the Bergell tonalite aureole. Am. J. Sci., 272: 423–437.

Trommsdorff, V. and Evans, B.W., 1977. Antigorite-ophicarbonates: contact metamorphism in Valmalenco, Italy. Contrib. Mineral. Petrol., 62: 301–312.

Trommsdorff, V. and Nievergelt, P., 1983. The Bregaglia (Bergell) Iorio Intrusive and its field relations. Mem. Soc. Geol. Ital., 26: 55–68.

Villa, I.M. and von Blanckenburg, F., 1991. A hornblende 39Ar–40Ar age traverse of the Bregaglia tonalite (Southeast Central Alps). Schweiz. Mineral. Petrogr. Mitt., 71: 73–87.

Wenk, H.R., 1973. The structure of the Bergell Alps. Eclogae Geol. Helv., 66: 255–291.

Wenk, H.R., 1992. Explanatory Note for Geologischer Atlas der Schweiz. 1:25000, Blatt 70 Sciora. Swiss Geol. Comm.

Wenk, H.R. and Cornelius, S.B., 1977. Geologischer Atlas der Schweiz. 1:25000, Blatt 70 Sciora, Swiss Geol. Comm.